**Discover** Water

Research

# Flood risk assessment under the shared socioeconomic pathways: a case of electricity bulk supply points in Greater Accra, Ghana

**Ebenezer K. Siabi[1,6] · Akwasi Adu-Poku[2] · Nathaniel Oppong Otchere[2] · Edward A. Awafo[3] · Amos T. Kabo-bah[4] · Nana S. A. Derkyi[5] · Komlavi Akpoti[7] · Geophrey K. Anornu[8] · Eunice Akyereko Adjei[2] · Francis Kemausuor[2] · Mashael Yazdanie[9]**

Received: 22 March 2024 / Accepted: 1 October 2024
Published online: 07 October 2024


## Abstract
This study evaluates flood susceptibility and risk on Bulk Supply Points in the Greater Accra region (GAR) using a Frequency Ratio model based on 15 flood conditioning factors. The model explores the influence of natural, meteorological and anthropogenic factors on flooding occurrences under the Shared Socioeconomic Pathway (SSP) scenarios and assesses flood risks at Bulk Supply Points (BSPs). Flood susceptibility mapping was conducted for both current and future periods under various SSP scenarios. Results reveal that elevation, slope, soil type, distance from urban areas, and SPI are the most influential factors contributing to flooding susceptibility in the region. The current flood map, about 37% of the total area of GAR categorized under the moderate flood-susceptible zone category followed by about 30% categorized under the low flood-vulnerable zone. However, about 16% was categorized under the very high flood-vulnerable zone. The study projects increasing flood susceptibility under the SSP scenarios with intensification under SSP2 and SSP3 scenarios. For instance, the areas categorized as high and very high flood susceptibility zones are projected to expand to approximately 32% and 26% each by 2055 under SSP3. The study also assesses flood risks at Bulk Supply Points (BSPs), highlighting the escalating susceptibility of power assets to flooding under different scenarios. For instance, in the very high scenario, flooding is estimated to reach 640 h in 2045 and exceed 800 h in 2055—more than double the 2020 baseline. The analysis shows the bulk supply points face increasing flood susceptibility, with risks escalating most sharply under the severe climate change SSP3 and SSP5 scenarios. Over 75% of BSPs are expected to fall in the low- to medium-risk categories across SSPs while more than 50% of BSPs are within medium- to high-risk categories in all scenarios except SSP1, reflecting the impact of climate change. SSP3 and SSP5 stand out with over 60% of BSPs facing high or very high flooding risks by 2055. It indicates moderate resilience with proper adaptation but highlights potential disruptions in critical infrastructure, such as BSPs, during persistent flooding. The findings of the study are expected to inform Ghana's contributions towards addressing Sustainable Development Goals (SDGs) 7, 11 and 13 in Ghana.

✉ Ebenezer K. Siabi, ebenezer.siabi@uenr.edu.gh; ✉ Mashael Yazdanie, Mashael.Yazdanie@empa.ch | [1]Earth Observation Research and Innovation Center (EORIC), University of Energy and Natural Resources, P.O. Box 214, Sunyani, Ghana. [2]The Brew Hammond Energy Center, Kwame Nkrumah University of Science and Technology, Kumasi, Ghana. [3]Department of Agricultural and Bioresources Engineering, University of Energy and Natural Resources, P. O. Box 214, Sunyani, Ghana. [4]Department of Civil and Environmental Engineering, University of Energy and Natural Resources, P. O. Box 214, Sunyani, Ghana. [5]Department of Renewable Energy Engineering, University of Energy and Natural Resources, P. O. Box 214, Sunyani, Ghana. [6]Regional Center for Energy and Environmental Sustainability, University of Energy and Natural Resources, P. O. Box 214, Sunyani, Ghana. [7]International Water Management Institute (IWMI), Accra, Ghana. [8]Department of Civil Engineering, Kwame Nkrumah University of Science and Technology, Kumasi, Ghana. [9]Urban Energy Systems Laboratory, Empa, Swiss Federal Laboratories for Materials Science and Technology, Überlandstrasse 129, 8600 Dübendorf, Switzerland.



Discover

**Keywords** Flood modeling · SSPs · Buly supply points · Flood risk · Sustainable development · Frequency ratio · Flood susceptibility

## 1 Introduction

Over the years, various forms of natural and anthropogenically-induced disasters, such as earthquakes, landslides, hurricanes, volcanic eruptions, and floods, amongst others, have occurred [1–3]. Floods are natural disasters caused by an overflow of a large volume of water above its usual limits, resulting in temporary inundation of river banks and stagnant water [4]. It is one of the most common types of natural/man-made disasters that interrupts anthropogenic activities, destroys properties and causes loss of life. Moreover, floods are known to destroy environmental ecosystems, disrupt agricultural activities and socio-cultural hereditament [5–9]. Globally, floods are noted to be a tragic and sudden event, resulting in huge wealth and health losses.

Sarkar and Mondal [4] noted that from 1963 to 1992, floods had caused about 32% of damage to the environment and humans. Currently, floods have resulted in the loss of 100,000 lives globally, affecting approximately 2 billion people and causing damages estimated at around $651 billion [10]. The African continent is the second-most vulnerable continent to floods after Asia in terms of the frequency of events, magnitude of affected areas and lives lost [11, 12]. Most countries in Africa have had a taste of awful flood-related disasters in the recent past. For instance, Mozambique recorded one of the most devastating floods in February and March 2000 amongst flood events in the last 50 years [13]. Again, the 2007 flood event which affected countries such as Togo, Mali, Burkina Faso, Niger, Uganda, Sudan and Ethiopia killed more than 500 people while displacing several millions of inhabitants [14].

The UN regional Coordinator in Dakar revealed that the July 2007 flood event in West Africa was the most tragic flood event in the last 30 years. As a result of the flood event, more than 210,000 and 785,000 people were killed and displaced, respectively. Again, about 600,000 inhabitants were affected after torrential rains in 16 Wwest African countries where Ghana, Burkina Faso, Niger and Senegal were the most affected. Aside from this, Nigeria in 2012 recorded one of the most catastrophic flood events ever observed, which resulted in the displacement and death of 2.3 million and 363 people, respectively [15].

The existence of perennial urban flooding in Ghana dates back to 1930 [16]. At least about 18 out of the last 50 years have observed substantial flood events where properties and lives have been lost [16–19]. The study of Douglas et al. [13] revealed that the occurrence of flood events in the coastal areas of Ghana has increased since 1995, resulting in the displacement and death of about 34,076 and 14 people, respectively. This also led to the property losses of about $168,289, as estimated by the National Disaster Management Organization (NADMO) [1].

Flooding has a significant impact on power systems. It can lead to long outage times and the destruction of power system equipment such as substations, transmission lines, and power plants [20]. In recent years, flooding has had devastating impacts on power infrastructure in many parts of the world, often leaving large populations without electricity for extended periods [21–23]. The Greater Accra region of Ghana has experienced several major flood events in the past decade, which have damaged key power assets and caused widespread blackouts across the capital city of Accra and surrounding areas [1, 24]. With climate change projections indicating increased variability and severity of extreme rainfall events in West Africa [7], there are growing concerns about the resilience of Ghana's power sector infrastructure to future flooding.

Flooding is of particular concern for the bulk supply points (BSPs) that deliver electricity from generating plants to end users in the Greater Accra region. These facilities, operated by the Ghana Grid Company (GRIDCo), contain vital transformers, switching gear and control equipment. Flood damage to BSPs can disrupt the entire downstream supply chain, affecting hospitals, businesses, homes, and other critical services. In 2015, major flooding of a GRIDCo substation in Achimota left many parts of Accra without power for several days [1]. With a growing population and electricity demand, along with the country's dependence on hydroelectric generation, Ghana's power sector is vulnerable to increases in extreme precipitation and flooding resulting from climate change. Therefore, this article examines the current and future flood risks facing the bulk supply point (BSPs) in the Greater Accra region. It assesses the exposure and susceptibility of these power infrastructures while exploring potential adaptation strategies to enhance resilience against future climate change impacts.

Therefore, mapping flood susceptibility to design management schemes can combat the destruction of BSPsin the future and be used to direct governments and policymakers to establish appropriate flood management strategies.

Geographical information system (GIS) and remote sensing (RS) techniques now have the capacity to support a new understanding of the assessment of susceptibility with better justification [4]. The analysis of satellite images through GIS and RS offers promising results for flood susceptibility mapping as it reveals flawless information about a specific area [25]. Several studies have successfully employed GIS and RS techniques in flood susceptibility assessment with different models [26–28]. The Frequency ratio (FR) model is a widely used technique with high overall accuracy [29]. The FR model uses bivariate statistical analysis to assign values to each class of each parameter and estimate its impact on flood occurrence [3, 29]. GIS and RS software offers a straightforward approach for mapping flood susceptibility using FR.

Other studies have employed various robust methodologies to map flood susceptibility. For instance, previous studies [30–34] utilized the Analytical Hierarchy Process (AHP) effectively in their flood susceptibility mapping efforts. Additionally, the Multi-Criteria Decision Support Approach (MCDA) has been implemented by [31, 35, 36]. Other methodologies like Weights of Evidence (WofE) as seen in Rahmati et al. [9], adaptive neuro-fuzzy interface systems such as Sezer et al. [37], and artificial neural networks (ANN) like those used by Tiwari & Chatterjee [38] have also been applied in various studies. While AHP remains the most commonly utilized approach, it is constrained by uncertainties stemming from user-provided information [39]. MCDA, on the other hand, is valued for its utility in flood mapping in data-scarce regions, often employed by local planners [40]. ANN attempts to establish relationships between flood conditioning factors and outcomes, yet its reliance on user inputs can introduce uncertainties in its predictions [41]. Recently, approaches like FR and WofE have emerged in flood susceptibility mapping, although they have predominantly been applied in other natural hazard mappings such as landslide studies [9, 42–44].

Several studies have generally mapped flood susceptibility in the Greater Accra region. However, most of these studies were limited to only the Accra metropolitan area. For example, Dekongmen et al. [45] studied flood vulnerability in Accra by analyzing natural factors like elevation, drainage density, and slope. However, their focus was restricted to these factors within the Accra metropolis alone, excluding the broader region. Similarly, other studies by [17, 36, 46–48] concentrated on flood susceptibility mapping specifically within the Accra metropolitan area. In contrast, Kwang and Osei [30], Njomaba et al. [49], and Kumi-Boateng [31] extended their investigations to cover almost the entire Greater Accra region, except for the Ada East and West districts. Nevertheless, these studies primarily mapped current flood susceptibility and did not include future flood projections under different climate scenarios, such as the Shared Socioeconomic Pathway scenarios (SSP), which remain largely unexplored in the region. Moreover, there are limited or no studies on the impacts of floods on bulk power supply points in Ghana's Greater Accra region. This presents a unique gap to investigate the impacts of flooding on BSPs and their related effects on power denial under the shared socio-economic pathway (SSP) scenarios. The findings of this study are expected to add knowledge to existing studies on the impacts of flooding in Greater Accra, especially on BSPs. Moreover, the findings of this study are expected to inform future adaptation strategies of different organizations, such as electricity distribution companies, NADMO and the various assemblies in different districts to manage floods under different scenarios better. Finally, the findings are expected to inform Ghana's contributions towards addressing Sustainable Development Goals (SDGs) 7, 11 and 13 in Ghana.

## 2 Materials and methods

### 2.1 Description of the study area

Greater Accra spans approximately 3,245 km$^2$ and is home to around 5,455,692 people according to the Ghana Statistical Service [50]. Positioned between Latitude 5°30′ to 5°53′ North and Longitude 0°03′ to 0°25′ West, this area exhibits occasional hills and lowlands, averaging about 20 m above sea level. The terrain generally maintains gentle slopes of about 11%, except for specific areas like Abokobi, Kwabenya, and the McCarthy hills, where slopes can exceed 22%. The water table in Greater Accra is situated between depths of 4.80 to 70 m below the surface [46]. Within the anomalous dry equatorial climatic region, Greater Accra experiences dual peaks of precipitation and a prolonged dry season, occasionally marked by dry Harmattan conditions. February and March are the hottest months, averaging around 27 °C monthly [50]. Conversely, the coldest months fall between June and August, with an average monthly temperature of approximately 21 °C (Ghana Statistical Service, 2014). Precipitation is characterized by two peaks: a major season from March to July and a minor one from September to November, totaling an annual precipitation range of 780–1200 mm [51], while the Ghana Meteorological Agency reports an average precipitation of about 812 mm [51]. Vegetation in the studied area comprises two primary types: coastal scrub and grasslands, alongside mangrove forests. The coastal scrub and grasslands, observed in specific Greater Accra locations, feature intermittent tree patches, including Baobab and

Neem trees. Mangrove forests, found in coastal lagoon areas with salty and waterlogged soil, delineate a distinct habitat. Figure 1 displays a map of the studied area.

In the Greater Accra region, flooding is a recurring concern, particularly in low-lying areas and zones with poor drainage systems. Heavy rainfall during the peak seasons, compounded by the region's topography and land use, often leads to inundation and waterlogging. The lack of adequate infrastructure and urban planning exacerbates this issue, making some areas prone to flash floods and subsequent damage to property and livelihoods. Additionally, the encroachment on waterways and wetlands further contributes to the region's susceptibility to flooding incidents. Addressing these challenges requires comprehensive flood mitigation strategies, improved drainage systems, and sustainable urban development practices to minimize the impact of flooding in Greater Accra.

## 2.2 Data sources and flood conditioning factors

The detailed specifications of the datasets used in the study are presented in Table 1, showing various types and sources. These datasets were used in generating layers of flood conditioning factors utilized in the FR model. Future precipitation data for different SSP scenarios in Greater Accra was sourced from the study of Siabi et al. [51]. Land use and land cover (LULC) changes under SSP scenarios were modeled using the GeoSOS-FLUS [52] software, based on the 2020 LULC map for Greater Accra. GeoSOS-FLUS integrates natural and human influences for simulating multi-type land use scenarios. Urban data, both current and future under SSP scenarios, were extracted from the respective LULC maps. Stream data was derived from the Shuttle Radar Topographic Mission (SRTM) digital elevation model (DEM) data, while road data

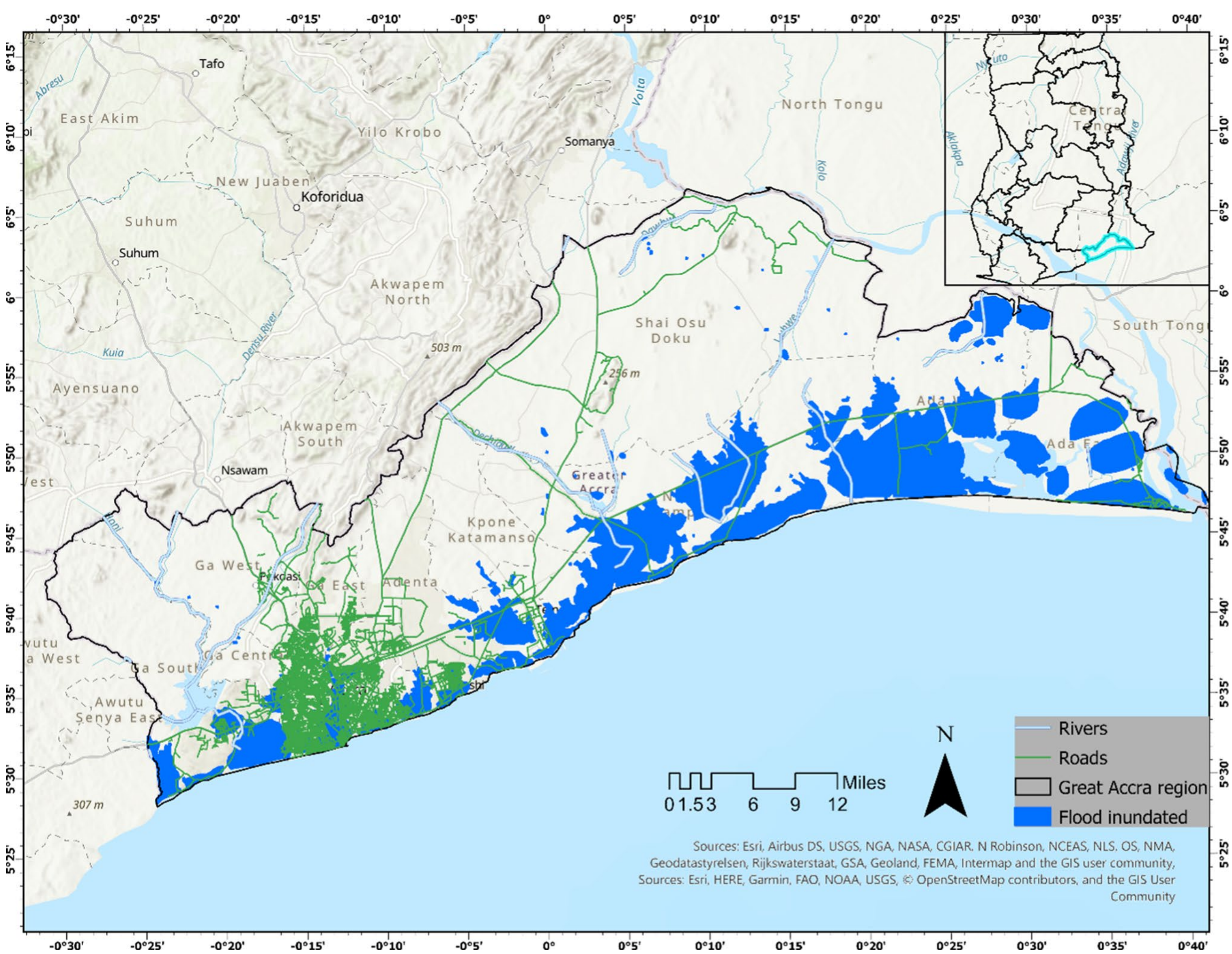


**Fig. 1** Study area map

**Table 1** Sources and type of data used

| Description of data | Data type/ resolution | Year | Source |
|---|---|---|---|
| Landsat 8 LULC map | 30 m | 2020 | Author generated |
| Future LULC | 30 m | 2020–2055 | Author generated |
| SRTM DEM | 90 m | 2020 | USGS |
| Stream | Raster | 2020 | Extracted from DEM |
| Geology | Raster | 2020 | Ghana Geological Survey Authority |
| Road | Raster | 2020 | Extracted from Google open street |
| Precipitation | Raster | 2020 | GMet |
| Future precipitation | Raster | 2020–2055 | Siabi et al. [51] |
| Urban data | Raster | 2020 | Retrieved from LULC map 2020 |
| Future Urban data | Raster | 2020–2055 | Retrieved from LULC maps 2020–2055 |
| Flood inventory data | Vector | 2015–2019 | NADMO/Literature/field survey [14, 17–19, 46, 55] |

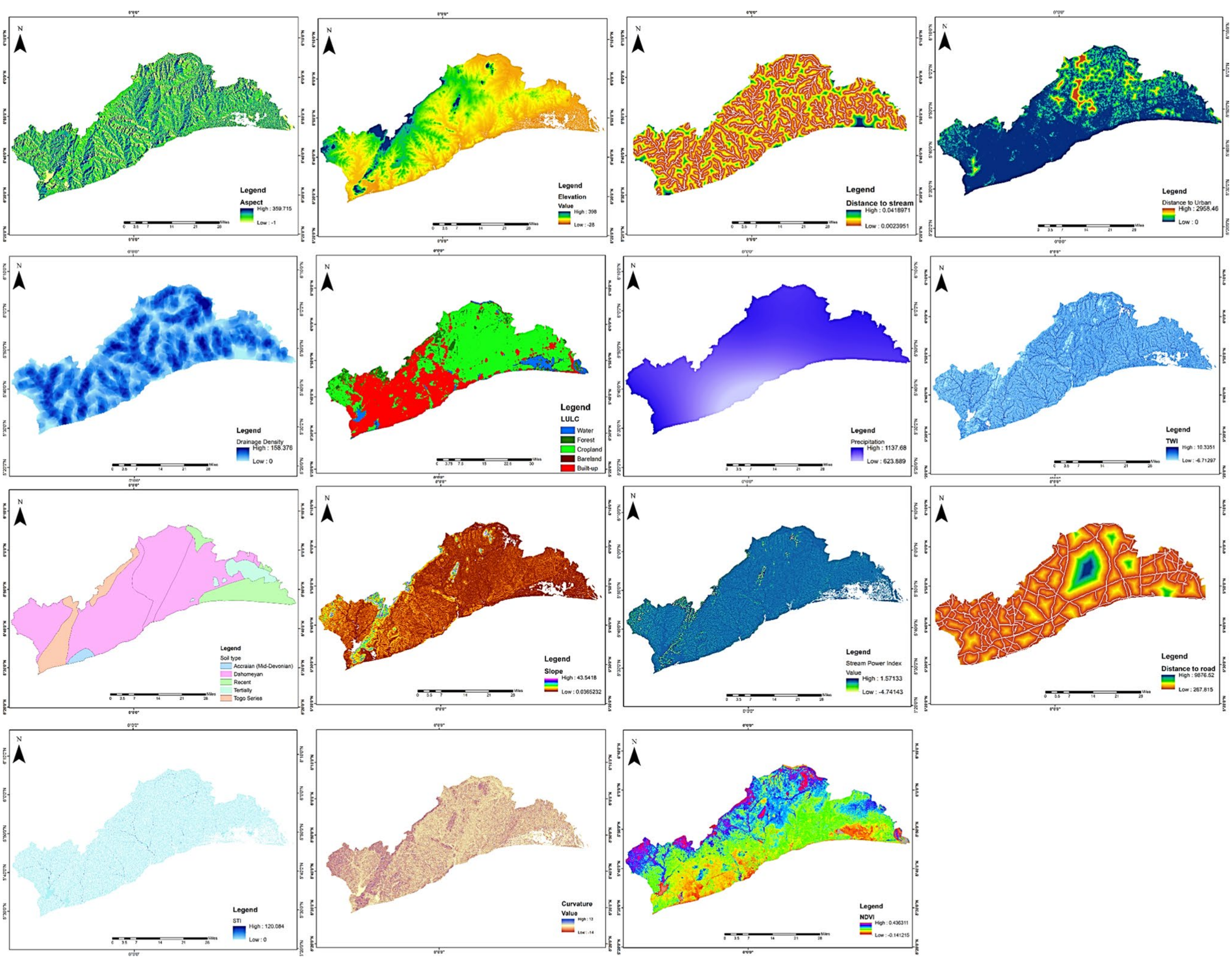

**Fig. 2** Flood conditioning factors used for the study

was obtained from Google Open Street Maps [53]. Elevation, slope, and topographic wetness index (TWI) were extracted from the SRTM DEM [54]. These datasets collectively formed the flood conditioning factors (Fig. 2).

#### 2.2.1 Elevation

Elevation is a key factor affecting flooding, with lower elevations generally experiencing a higher risk of flooding [54]. The study area, with elevations ranging from – 21 to 398 m above mean sea level (MSL), was divided into five elevation classes. Analysis of the elevation map indicates that the region predominantly consists of very low-lying areas within this range (Fig. 2). The predominance of these low elevations significantly contributes to the flood risk in the study area.

#### 2.2.2 Slope

Slope is a crucial factor in hydrology, with a direct relationship to surface runoff and a significant impact on flooding [55]. The slope of the study area, measured in degrees from the processed DEM, was reclassified accordingly. Typically, areas with low elevation feature gentle or flat slopes, making them more prone to flooding and waterlogging (Fig. 2). Steeper slopes, on the other hand, increase water velocity, leading to faster runoff. Conversely, flat or gently sloping terrain allows runoff to disperse more gradually [56]. As a result, low-gradient slopes in lower elevations are more susceptible to flooding compared to steeper, high-gradient areas. The elevation and resulting slope exhibit minimal spatial variation due to historical changes in the study area.

#### 2.2.3 Curvature

Curvature offers important insights into the terrain's geomorphological characteristics [57]. Plan curvature data, extracted from the DEM, was classified into three categories: concave, flat, and convex (Fig. 2). In the study area, 19.19% of the land has a concave curvature, 48.63% is flat, and 32.16% is convex.

#### 2.2.4 TWI (Topographic Wetness Index) and SPI (Stream Power Index)

TWI and SPI are critical hydrological factors commonly used in flood studies. TWI (Topographic Wetness Index) maps the spatial distribution of moisture, influencing surface runoff patterns [40], whereas SPI (Stream Power Index) measures the erosive potential of surface runoff [58].

#### 2.2.5 Soil type/Geology

In this study, geology is regarded as a key conditioning factor due to its direct impact on the ground's water absorption capacity [59]. Geological data for the region was sourced from the Ghana Geological Survey Authority. The study area includes five distinct geological units (Fig. 2), with Accranian geology being the most prevalent. Terrains with this geological composition are susceptible to rapid runoff, which heightens the risk of severe flooding downstream, especially during heavy rainfall events.

#### 2.2.6 Land use land cover

In susceptibility mapping, understanding the spatial distribution of Land Use and Land Cover (LULC) is crucial for identifying which land use types and activities are most affected by frequent flooding. Different LULC categories, such as croplands, bare lands, and built-up areas, particularly in low-lying regions, can significantly influence flood occurrence and severity. For instance, areas with extensive croplands may experience increased runoff due to soil disruption, while bare lands offer minimal absorption and can lead to heightened surface runoff. Built-up areas, especially in flood-prone zones, often have impervious surfaces that exacerbate flooding by preventing natural water absorption [3]. The LULC information for the study area, which highlights these factors, is detailed in Fig. 2. This information is vital for assessing flood risk and implementing effective land management strategies.

#### 2.2.7 Distance from stream and drainage density

Proximity to natural drainage is a critical conditioning factor due to its substantial impact on flooding. Areas located near natural drainage systems, such as streams and rivers, are more prone to flooding because these water bodies can quickly convey excess water during heavy rainfall. The distance from streams is an important aspect to consider; regions closer to streams are at a higher risk of flooding compared to those further away. This is because the closer proximity allows for less time for water to dissipate, leading to quicker accumulation and higher flood risks in these areas. Drainage density, which measures the extent of stream networks within the study area, also plays a crucial role in flood events. A higher drainage density, with numerous and densely packed streams, can exacerbate flooding by increasing the volume and speed of surface runoff. Areas with a high drainage density often experience more frequent and severe floods due to the efficient and rapid channeling of water from rainfall into streams and rivers. Figure 2 provides a detailed map showing both the distances from streams and the drainage density across the region. This information is essential for understanding how proximity to natural drainage and drainage density contribute to flood risk, aiding in the development of effective flood management strategies.

#### 2.2.8 Distance from urban and roads

The distance from urban areas and roads is a vital factor in assessing flood susceptibility in the Greater Accra region of Ghana. Urbanization significantly alters the region's hydrological dynamics, influencing its susceptibility to flooding. Analyzing how proximity to urban centers and transportation networks affects flood risk is essential for effective flood risk management and mitigation. Urbanization tends to increase flood risks through multiple mechanisms. The expansion of built-up areas does not only result in more impervious surfaces, but also lead to issues such as improper solid waste disposal into drainage systems, which can clog and impair their functionality, construction activities, especially in or near waterways, can further disrupt natural water flow and exacerbate flooding as well as informal activities in unplanned urban areas—such as unauthorized encroachments, and illegal dumping can severely affect drainage systems and water flow patterns. These activities can redirect or concentrate runoff towards areas not adequately prepared for high volumes of water, increasing the likelihood of severe flooding. Figure 2 shows the spatial distribution of distances from urban areas and roads.

#### 2.2.9 NDVI

In evaluating flood susceptibility, the Normalized Difference Vegetation Index (NDVI) is crucial for assessing land cover and land use changes. NDVI values range from − 1 to 1, with higher values reflecting healthier and denser vegetation (Fig. 2). Healthy vegetation, indicated by elevated NDVI values, enhances soil stability through root systems that bind the soil, reduce erosion, and improve water absorption. In flood-prone areas, robust vegetation can help mitigate the effects of heavy rainfall by promoting natural drainage and reducing surface runoff. NDVI is also instrumental in identifying and delineating floodplains. Areas with lower NDVI values, such as barren land or urbanized regions, typically exhibit reduced vegetation density and may be more vulnerable to flooding. By incorporating NDVI data into floodplain mapping, authorities can better identify high-risk areas and implement targeted flood mitigation strategies. This integration supports more effective flood management by highlighting areas where vegetation can play a critical role in flood prevention and management.

#### 2.2.10 Aspect

The aspect, or the direction a slope faces, is a key factor in flood susceptibility within the region of Ghana (Fig. 2). Analyzing the aspect of terrain offers important understandings into water runoff patterns and their impact on flooding risk and also identify how different slope orientations affect water accumulation and runoff behavior. For example, low-lying areas with certain slope aspects may be more prone to water accumulation, especially during heavy rainfall. Conversely, slopes oriented in directions that facilitate rapid runoff can increase the likelihood of flash floods in downstream areas. Therefore, evaluating aspect data is crucial for identifying areas at greater risk of flooding and for implementing appropriate flood management strategies.

### 2.3 Flood inventory

For flood susceptibility mapping, it is imperative to consider historical flood occurrence data that is scientifically justified to forecast future floods [60]. The accuracy and reliability of the forecasted flood susceptibility rely on the correctness of historical flooding events [4]. Flood inventory data from 2015 to 2019 was obtained from the field survey, NADMO and literature [14, 17–19, 46, 61]. The study used a sum of 384 flood points. These points were randomly divided into training and validation of the developed flood model; 70% and 30% of the flood points were used for training and testing the final model, respectively. Several studies have employed this same structure in the training and authentication of their models [8, 9, 60]. However, there are no specific rules for defining how flood points are divided into training and validation [29]. Figure 3 presents the flood inventory map of the Greater Accra region.

### 2.4 Frequency ratio model

The evaluation of flood susceptibility is relevant to discover the conditioning factors of floods. The association between the occurrence of flooding and the related conditioning factors can be detected based on historical flooding events and their causative factors. The study utilizes the FR model in generating the flood susceptibility maps for Greater Accra under the SSP scenarios. The FR model is a bivariate statistical analysis technique that critically analyzes the contribution of each

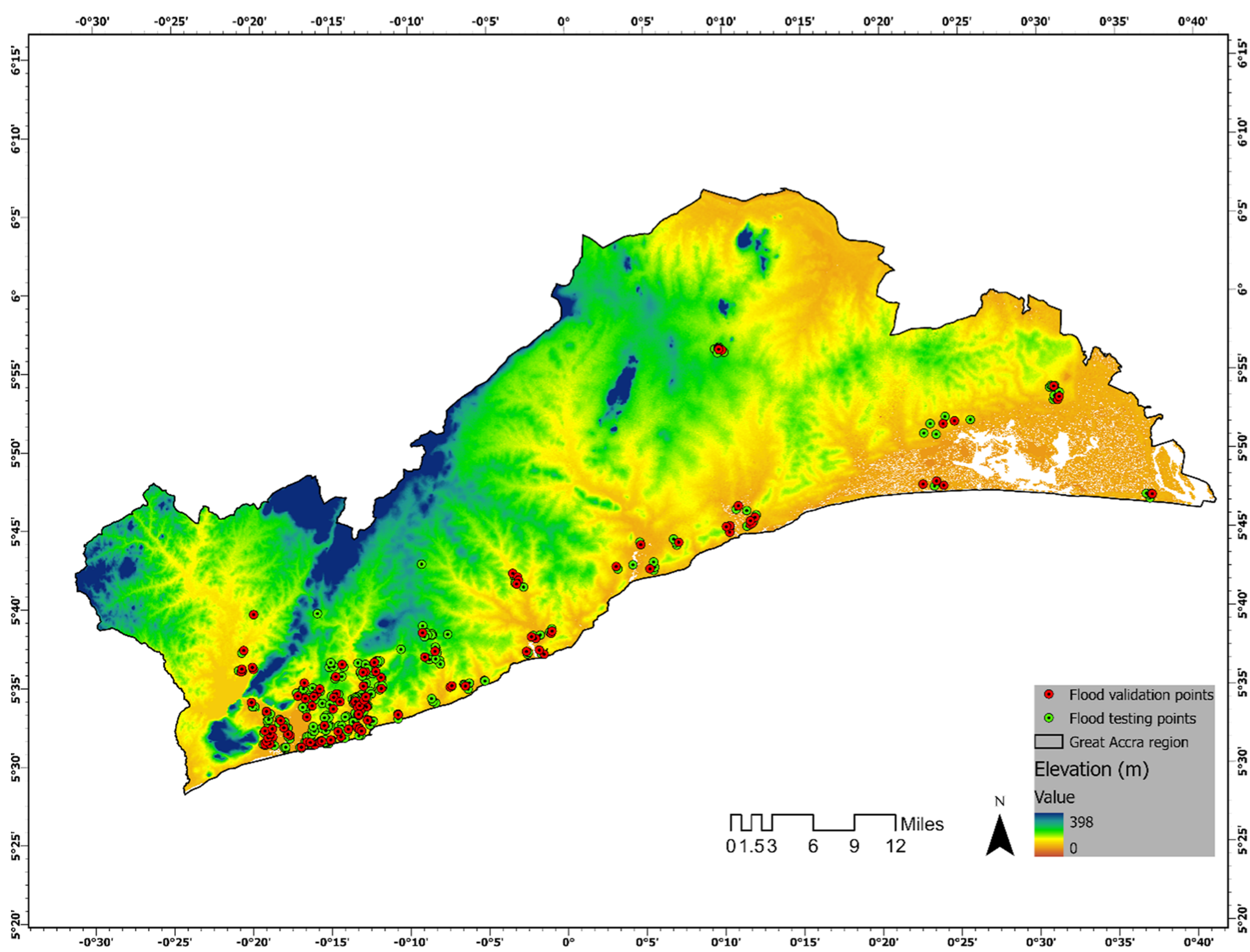


**Fig. 3** Greater Accra Flood inventory map

class of each flood conditioning factor on future flooding [30]. FR (see Eq. 1) is estimated by analyzing the association between flood events and the contributing factors. Therefore, FR [62, 63] is given as:

$$FR = \frac{\left[\frac{N_{pix}(X_i)}{\sum_{i=1}^{m} X_i}\right]}{\left[\frac{N_{pix}(X_j)}{\sum_{j=1}^{n} N_{pix}(X_j)}\right]} \tag{1}$$

where $N_{pix}(X_i)$ = number of flood points in class $i$ of variable X; $N_{pix}(X_j)$ = the number of pixels in variable $X_j$; $m$ = total classes in the variable $X_i$; $n$ = total factors of the study area.

An FR value greater than 1 indicates significant parameters that strongly contribute to flooding. Conversely, an FR value less than 1 signifies an inverse relationship between flood occurrence and the conditioning factors [41, 64–67].

After the estimation of the FR for every class, all values for each conditioning factor are summed for generating the final flood susceptibility map. The formula for the final flood susceptibility index (FSI) (see Eq. 2) is given as:

$$\mathrm{FSI} = \sum_{j=1}^{n} \mathrm{FR} \tag{2}$$

The FR approach has been successfully applied for flood susceptibility mapping globally [4, 8, 9, 26].

However, prediction rate is calculated as

$$= \left(\mathrm{Max\,RF}^{i} - \mathrm{Min\,RF}^{i}\right) - Q$$

where RF = relative frequency and defined as the FR value per class divided by the sum of FR values for an input parameter; Max $\mathrm{RF}^{i}$ = the Maximum relative frequency value of ith parameter; Min $\mathrm{RF}^{i}$ = the Minimum relative frequency value of ith parameter; Q = the lowest difference $(MaxRF^{i} - MinRF^{i})$ attained by an input parameter compared to all other parameters.

### 2.5 Model validation

The receiver operating characteristic (ROC) curve [68] was used to validate the baseline flood susceptibility map. The ROC curve is a scientific and general technique of assessing the accuracy of a model. In the ROC curve, the X and Y axes show the false and true positive rates, respectively. To substantiate the prediction of models, the area under the curve (AUC) is considered. An AUC value of less than 0.50 is considered unsatisfactory for flood susceptibility mapping. A perfect model is attained when the AUC is 1. Therefore, the model is defined as poor when the AUC is between 0.5 and 0.6. The model is good when the AUC is between 0.7 and 0.8, and the model is very good and excellent when AUC is between 0.8–0.9 and 0.9–1, respectively.

### 2.6 Methodological roadmap for the flood susceptibility mapping

Figure 4 shows the methodological roadmap for generating current and future flood susceptibility maps of Greater Accra. The flood conditioning factors were categorized into natural and anthropogenic factors. The preprocessing stage initially involved clipping and reclassifying all datasets to the study area into five subclasses. Subsequently, thematic layers were created for each factor, all standardized to a spatial resolution of 30 m, consistent with the LULC data resolution. A flood inventory map was developed using historical flood data sourced from field surveys, NADMO, and literature (Table 1). This, combined with future layers such as distance from urban areas, precipitation, and LULC under SSP scenarios, constituted the input data for the FR model (see Fig. 2). The baseline flood susceptibility map generated by the FR model was validated and assessed for performance using Receiver Operating Characteristic-Area under the curve (ROC-AUC). If the model performed well, future flood susceptibility maps were produced. If performance was inadequate, the model underwent recalibration until satisfactory validation scores were achieved. For forecasting future floods under SSP scenarios, all flood conditioning factors were kept constant except for variable factors like precipitation, LULC changes, and distance from urban areas (Table 1).

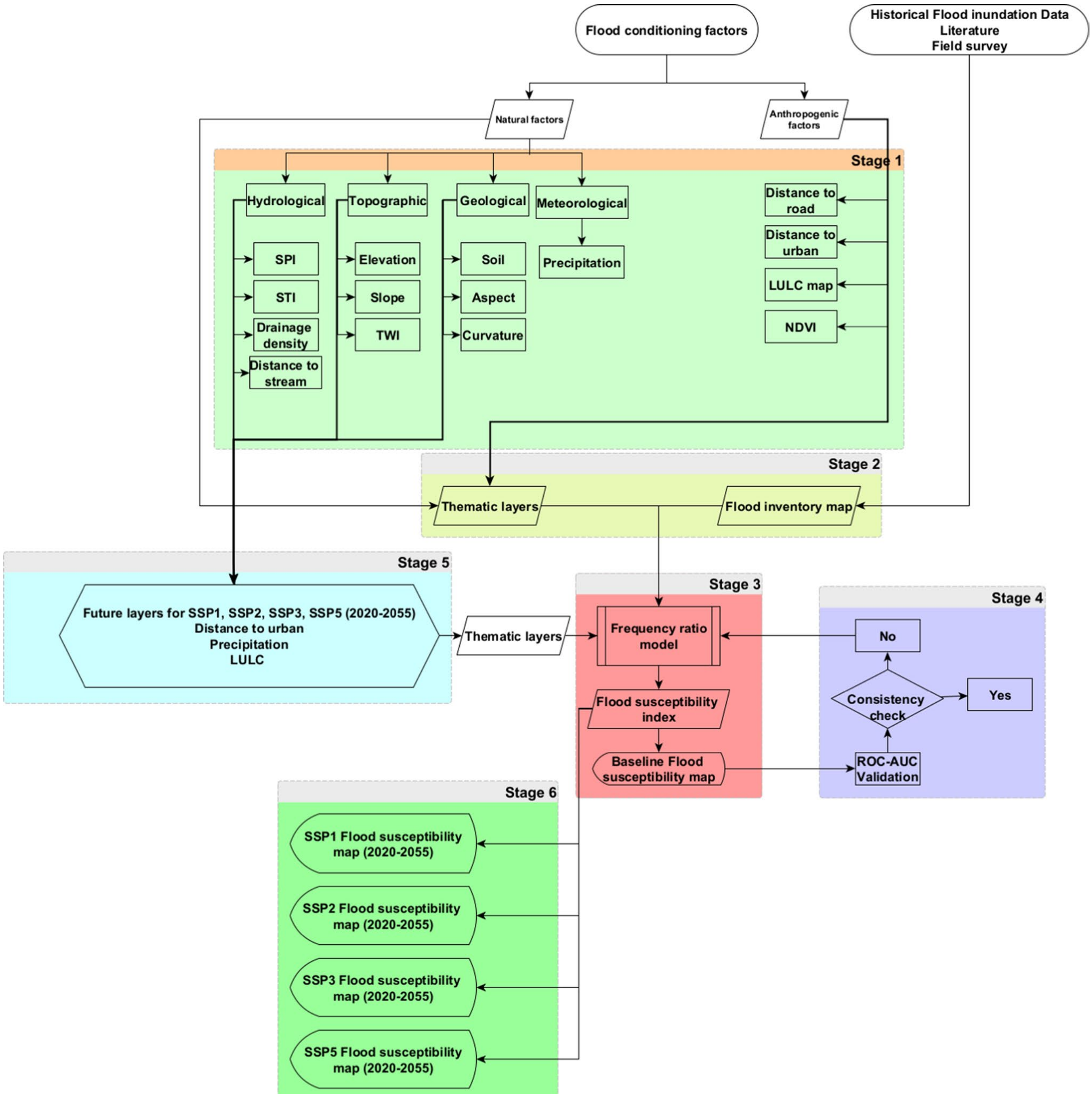


**Fig. 4** Methodological flowchart for flood susceptibility mapping

## 2.7 Flood exposure analysis

Historical precipitation data from 1991 to 2020 was obtained from the World Climate Guide to determine average monthly rainfall days in Accra [69]. A typical 8-h flooding duration from a heavy rainfall event was estimated based on prior hydrologic analysis by Ansah et al. [70]. This 8-h duration was adjusted by ± 2 h to represent moderate and very heavy rainfall events, respectively, according to USGS rainfall intensity classifications [71].

Future rainfall intensification under each SSP scenario was quantified using the prediction rates of influential flood conditioning factors (precipitation, land cover, and distance from urban areas) from the frequency ratio flood model results. The relative increase in these factors compared to 2020 baseline levels was used to scale the typical 8-h flooding duration each month and estimate future flood duration hours through to 2055.

### 2.8 Annual electricity supply potential

The locations of 45 electricity bulk supply points (BSPs) in Greater Accra were mapped in GIS software using data obtained from GRIDCo and the Electricity Company of Ghana (ECG), as presented in Appendix 3. The capacity and average annual availability of each BSP facility were compiled based on information from the electricity distribution companies. Availability factors of 0.85 accounting for maintenance downtime were applied to estimate each BSP's annual electricity supply potential in MWh based on its capacity in MW.

$$\text{Supply(MWh)} = \text{Capacity(MW)} \times \text{Operating time(h)} \times \text{Availability factor}(\%) \tag{3}$$

### 2.9 Power denial estimation

We define power denial in this context to mean power not available to consumers due to the shutdown of a flooded BSP. Flood susceptibility maps were used to identify BSP susceptibility to flood which is crucial for a comprehensive risk assessment. While flood depth and duration are primary factors in determining potential inundation, the use of flood susceptibility maps provided additional critical insights by incorporating multiple flood conditioning factors such as elevation, land cover, and drainage density. This multidimensional approach enhanced the predictive accuracy of flood risks, which informs strategic planning for infrastructure resilience under different climate scenarios. The flood duration estimated each month per SSP scenario were assumed to represent BSP outage times during an extreme flooding event to quantify power denial in Eq. (4). The outage time was multiplied by the capacity to estimate power denial in MWh for each BSP (see Appendix 3). Results were summed across all BSPs to determine total power denial in Greater Accra under each future flooding scenario.

$$\text{Power denied (MWh)} = \text{Capacity (MW)} \times \text{Outage time (h)} \tag{4}$$

## 3 Results

### 3.1 FR values for flood conditioning factors

Table 2 presents the weights of the various sub-classes of the 16 flood conditioning factors used in the FR model. FR values for flood conditioning factors, such as elevation, slope, precipitation, TWI, STI, SPI, and drainage density, have been estimated using the FR model (see Appendix 1). High SPI values between 0.21–0.04 and 0.03 – 1.57 had FR values that are considerably greater than one (Table 2). This implies that, the higher SPI the higher the probability of occurrence of flood. Similarly, FR values tend to increase as precipitation increases. For instance, precipitation subclasses between 948–1018 mm (FR = 1.13) and 1018–1137 mm (FR = 1.06) recorded FR values that are greater than one (see Table 2). This signifies high probability of flood occurrence in high rainfall areas of the region.

For distance from stream, areas with distance between 0.0024 and 0.0053 m to stream recorded an FR value of 1.34. This signifies that as the distance decreases from a stream, the FR value increases leading to a high probability of flooding in these areas. Likewise, FR values tend to increase as distance from urban areas decreases. For instance, areas with distance between 1–72.56 and 72.56–141.87 m from urban recorded 1.08 and 1.33 FR values, respectively, showing a high probability of flooding in these areas (Table 2). Distance from urbanization is one of the major contributors of flooding events. Urban areas are known for their concretization, which prevents rainwater from seeping into the ground; as a result, surface runoff is accelerated, leading to flooding in areas where draining systems are not big enough to handle the flow accumulation.

From Table 2, the FR values are more than one where NDVI is between − 0.14 and 0.15, signifying no or unhealthy vegetation with higher chances of flooding (see Table 2). NDVI, which shows the health of vegetation, may contribute to flooding since areas where there is no or unhealthy vegetation has a greater chance for flooding. Moreover, LULC sub-classes such as water (FR = 1.94), cropland (1.04) and bareland (2.03) had FR values that is more than 1, compared to

**Table 2** Features and FR results of flood factors

| Factors | Classes | Total pixel ($km^2$) | % of area | Total flood pixel ($km^2$) | % of area | FR |
|---|---|---|---|---|---|---|
| Stream Power Index (SPI) | – 4.74 to 1.42 | 1049 | 0.261 | 4 | 0.004 | 0.016 |
| | – 1.42 to 0.61 | 4990 | 1.239 | 55 | 0.057 | 0.046 |
| | 0.61–0.21 | 41,711 | 10.360 | 6798 | 7.089 | 0.684 |
| | 0.21–0.04 | 179,819 | 44.664 | 45,555 | 47.508 | 1.064 |
| | 0.03–1.57 | 175,033 | 43.475 | 43,478 | 45.342 | 1.043 |
| Precipitation (mm) | 623.88–762.91 | 30,324 | 7.067 | 13,758 | 3.471 | 0.491 |
| | 762.91–861.64 | 45,998 | 10.720 | 11,769 | 9.024 | 0.842 |
| | 861.64–948.28 | 67,467 | 15.724 | 14,759 | 15.481 | 0.985 |
| | 948.28–1018.80 | 98,925 | 23.055 | 28,333 | 26.172 | 1.135 |
| | 1018.80–1137.67 | 186,369 | 43.434 | 39,638 | 45.852 | 1.056 |
| Distance from stream (m) | 0.022–0.042 | 6266 | 1.657 | 1975 | 1.090 | 0.658 |
| | 0.015–0.022 | 41,034 | 10.848 | 5695 | 6.366 | 0.587 |
| | 0.01–0.015 | 81,857 | 21.641 | 13,274 | 14.838 | 0.686 |
| | 0.0053–0.01 | 110,640 | 29.251 | 24,687 | 28.713 | 0.982 |
| | 0.0024–0.0053 | 138,449 | 36.603 | 43,829 | 48.993 | 1.338 |
| Distance from urban (m) | 281.91–359.71 | 15,045 | 3.505 | 46 | 0.042 | 0.012 |
| | 209.77–281.91 | 26,932 | 6.274 | 714 | 0.658 | 0.105 |
| | 141.87–209.77 | 46,273 | 10.780 | 9189 | 8.471 | 0.786 |
| | 72.56–141.87 | 89,163 | 20.773 | 29,993 | 27.649 | 1.331 |
| | 1–72.56 | 251,818 | 58.667 | 68,537 | 63.180 | 1.077 |
| Normalized Difference Vegetation Index (NDVI) | 0.264–0.436 | 47,654 | 11.107 | 3962 | 3.649 | 0.329 |
| | 0.203–0.264 | 133,523 | 31.120 | 21,658 | 19.948 | 0.641 |
| | 0.150–0.203 | 141,812 | 33.052 | 45,587 | 41.987 | 1.270 |
| | 0.094–0.150 | 91,856 | 21.409 | 30,034 | 27.662 | 1.292 |
| | – 0.14 to 0.09 | 14,208 | 3.311 | 7334 | 6.755 | 2.040 |
| Landuse Land cover (LULC) 2020 | Water | 16,604 | 3.871 | 8153 | 7.517 | 1.942 |
| | Forest | 24,147 | 5.630 | 2402 | 2.215 | 0.393 |
| | Cropland | 225,280 | 52.525 | 59,228 | 54.608 | 1.040 |
| | Bareland | 2824 | 0.658 | 1447 | 1.334 | 2.026 |
| | Built-up | 160,047 | 37.316 | 37,230 | 34.326 | 0.920 |
| Drainage density | 59.06–99.74 | 89,984 | 20.980 | 16,781 | 15.576 | 0.742 |
| | 41.46–59.06 | 118,472 | 27.622 | 23,931 | 22.213 | 0.804 |
| | 26.99–41.46 | 101,969 | 23.774 | 25,596 | 23.758 | 0.999 |
| | 13.3–26.99 | 81,719 | 19.053 | 28,457 | 26.414 | 1.386 |
| | 0.001–13.3 | 36,765 | 8.572 | 12,970 | 12.039 | 1.404 |
| Slope | 16.03–43.54 | 1450 | 0.356 | 3 | 0.003 | 0.008 |
| | 8.40–16.07 | 5748 | 1.410 | 42 | 0.041 | 0.029 |
| | 3.62–8.40 | 16,065 | 3.940 | 456 | 0.450 | 0.114 |
| | 1.23–3.62 | 140,607 | 34.483 | 24,432 | 24.129 | 0.700 |
| | 0.036–1.23 | 243,887 | 59.812 | 76,324 | 75.377 | 1.260 |
| Curvature | – 13 to 2.02 | 6032 | 1.447 | 3 | 0.003 | 0.002 |
| | – 2.02 to 1.04 | 18,463 | 4.432 | 4 | 0.004 | 0.016 |
| | – 1.04 to 0.04 | 62,533 | 14.709 | 20,765 | 19.199 | 1.003 |
| | 0.04–1.02 | 209,269 | 49.456 | 52,594 | 48.635 | 1.024 |
| | 1.02–12 | 126,849 | 29.956 | 34,778 | 32.159 | 0.983 |

**Table 2** (continued)

| Factors | Classes | Total pixel (km$^2$) | % of area | Total flood pixel (km$^2$) | % of area | FR |
|---|---|---|---|---|---|---|
| Aspect | −1 to 73.56 | 68,811 | 16.700 | 14,819 | 14.141 | 1.141 |
| | 72.56–141.87 | 81,012 | 19.662 | 21,456 | 20.474 | 0.814 |
| | 141.87–209.77 | 87,322 | 21.193 | 24,747 | 23.615 | 0.847 |
| | 209.77–281.91 | 96,054 | 23.312 | 24,183 | 23.077 | 0.990 |
| | 281.91–359.71 | 78,833 | 19.133 | 19,589 | 18.693 | 0.977 |
| Topographic Wetness Index (TWI) | – 6.71 to 2.97 | 129,318 | 31.714 | 20,276 | 20.024 | 0.631 |
| | – 2.97 to 1.43 | 157,432 | 38.609 | 41,979 | 41.458 | 1.074 |
| | – 1.43 to 0.64 | 74,951 | 18.381 | 23,861 | 23.565 | 1.282 |
| | 0.64–3.58 | 33,695 | 8.264 | 10,523 | 10.392 | 1.258 |
| | 3.58–10.33 | 12,361 | 3.031 | 4618 | 4.561 | 1.504 |
| Elevation (m) | 194.53–437 | 6032 | 1.449 | 3 | 0.003 | 0.002 |
| | 113.71–194.53 | 18,463 | 4.434 | 6 | 0.006 | 0.001 |
| | 74.19–113.71 | 92,909 | 22.315 | 11 | 0.011 | 0.000 |
| | 47.25–74.19 | 168,402 | 40.447 | 7212 | 6.902 | 0.171 |
| | 21–47.25 | 130,544 | 31.354 | 97,260 | 93.079 | 2.969 |
| Soil | Togo series | 40,875 | 9.569 | 8899 | 8.286 | 0.866 |
| | Tertially | 48,469 | 11.347 | 5046 | 4.698 | 0.414 |
| | Dahomeyan | 80,320 | 18.803 | 6614 | 5.227 | 0.278 |
| | Accraian | 186,125 | 43.573 | 46,010 | 43.771 | 1.005 |
| | Recent | 71,372 | 16.708 | 40,830 | 38.017 | 2.275 |
| Distance to road (m) | 6033.04–9876.52 | 9836 | 2.533 | 67 | 0.070 | 0.028 |
| | 3621.44–6033.04 | 22,102 | 5.691 | 901 | 0.938 | 0.165 |
| | 2038.83–3621.44 | 51,748 | 13.325 | 12,120 | 12.624 | 0.947 |
| | 946.08–2038.83 | 111,092 | 28.605 | 29,550 | 30.779 | 1.076 |
| | 267.81–946.08 | 193,585 | 49.846 | 53,369 | 55.589 | 1.115 |
| Sediment Transport Index (STI) | 0–2.83 | 208,729 | 96.171 | 50,072 | 94.638 | 0.984 |
| | 2.83–12.24 | 6684 | 3.080 | 2018 | 3.814 | 1.238 |
| | 12.24–30.61 | 1208 | 0.557 | 532 | 1.006 | 1.807 |
| | 30.61–64.04 | 341 | 0.157 | 212 | 0.401 | 2.550 |
| | 64.04–120.08 | 77 | 0.035 | 75 | 0.142 | 3.996 |

forested area (0.39). LULC of an area is important to identify flood-prone areas in a river catchment. For instance, forest may act as natural resistance to flood prevention in an area. However, open fields and unprotected areas, such as water, crop and bare lands may be susceptible to flooding. Again, concretization in built-up areas results in an insignificant amount of groundwater percolation while aiding high surface runoff.

Concerning drainage density, areas with low drainage density have higher chances of flooding. For instance, areas with lower drainage density (< 27) in Greater Accra observed about 38% of historical flooding as FR values for subclasses between 0.001–13.3 and 13.3–26.99 were all above one (see Table 2). This reveals the susceptibility of these areas. Table 2 shows that areas between 0.036° and 1.23° slope subclass are prone to flooding as the FR value (1.26) is more than one. The slope of an area controls the occurrence of flooding, as low-lying areas have a significant relationship with flooding conditions in the rainy season. High numbers of flood events occur in lower slope regions as the water cannot discharge rapidly. Furthermore, curvature between – 1.04–0.04 and 0.04–1.02 produced FR values greater than 1. This shows that areas within these two classes are susceptible to flooding. Likewise, areas with Aspect between – 1 and 73.56 producing FR values greater than one.

The TWI and elevation are also important flood conditioning factors. Flood probability tends to increase where TWI increases. For instance, all the subclasses (except the first subclass) had FR values greater than one (see Table 2). However, flood probability increases when elevation decreases. Thus, FR values decrease when altitude increases and vice versa.

For instance, the FR value obtained for the lower elevated areas (21–47 m above sea level) recorded high FR value of 2.97. This reveals a significant impact of elevation on flood occurrence in the Greater Accra region. For soil, the Recent and Accranian soil types were found to influence the occurrence of flooding by producing FR values of 2.27 and 1 respectively. Moreover, Furthermore, the distance to a road between 267–946 m and 946–2038 m produced FR values of 1.12 and 1.08, respectively. This suggests that proximity to a road increases flood susceptibility in Greater Accra. Finally, all subclasses of STI, except the first subclass, produced FR values above one.

### 3.2 Mapping of flood susceptibility in Greater Accra

For preparing the flood-vulnerable maps, layers were created for all—15 flood conditioning factors and prediction rates estimated respectively. The prediction rate, which curbs issues of drawback and considers the mutual interrelationship among independent factors was estimated. The prediction rate reveals the sensitivity of individual flood conditioning factors with the training data. All the flood conditioning factors were combined for the baseline and future periods to generate flood susceptibility maps for the baseline period and under the SSP scenarios. For preparing the flood-vulnerable map for the baseline period, the results were categorized into 5 subclasses ranging from very low to very high. Figure 5 present the final flood susceptibility map. The prediction rate of flood conditioning factors (left) and percentage of flood vulnerable zones (right) are presented in Fig. 6. Elevation, slope, soil, distance from urban, and SPI were the first five most sensitive parameters that supported flooding in the Greater Accra region, with elevation being the most sensitive parameter (Fig. 6). About 37% of the total area of Greater Accra is categorized under the moderate

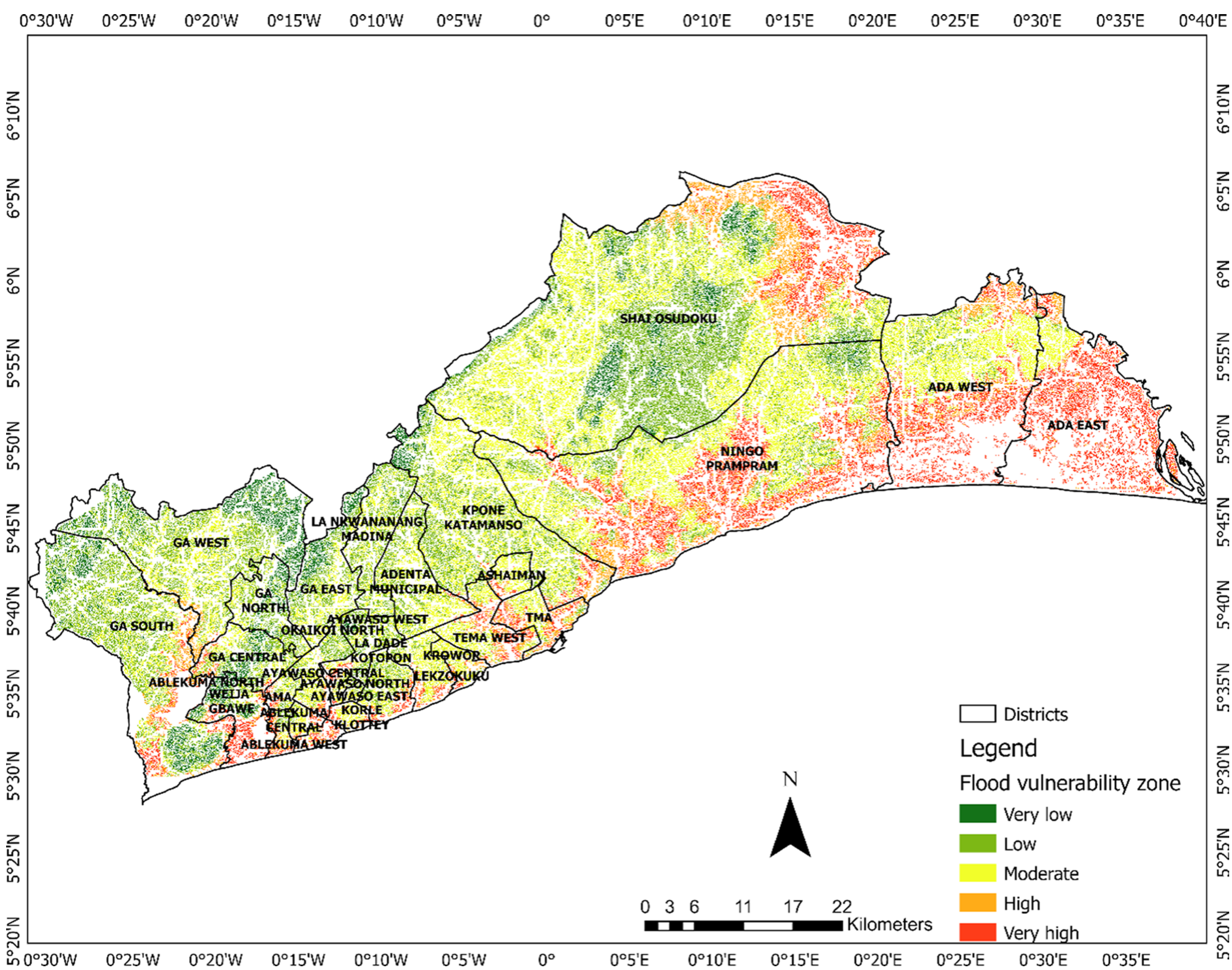


Fig. 5 Flood susceptibility map of Greater Accra region for the year 2020

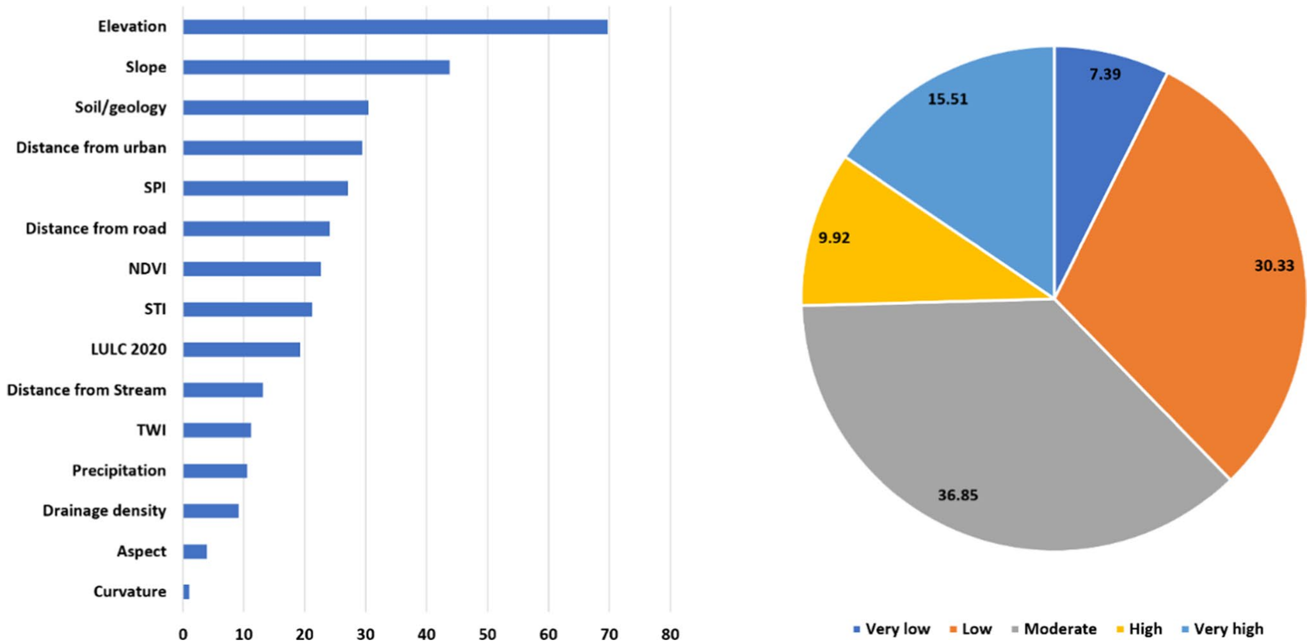


**Fig. 6** Prediction rate of flood conditioning factors used in the FR model (left) and percentage of flood susceptibility zones (right)

flood-vulnerable zone category (Fig. 6, right). This followed by about 30% categorized under the low flood-vulnerable zone. However, about 15.5% was categorized under the very high flood-vulnerable zone (Fig. 6, right). Districts such as Ga South, Accra Metropolis, La Dade-Kotopon, Ledzokuku-Krowor, Kpone Katamanso, Ningo Prampram, Ada West and Ada East had parts located in the very high flood susceptibility zone (see Fig. 5). All these areas are very low-lying and along

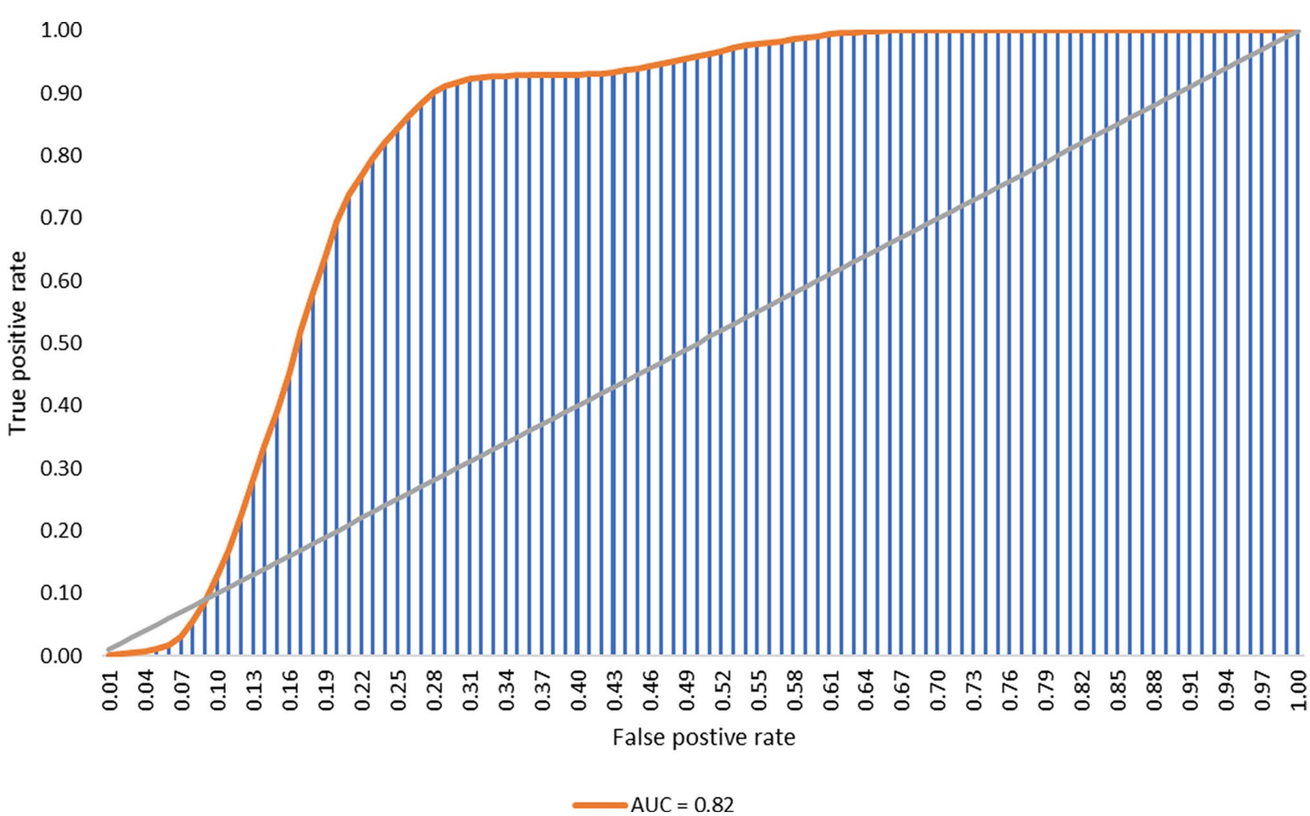


**Fig. 7** ROC curve of the FR model

the coastal regions of Greater Accra (Fig. 5). This reveals the susceptibility of low-lying and coastal areas to flooding. The present study attained an AUC value of 0.83 (see Fig. 7), which shows that the model is very good and accurate for flood susceptibility mapping for Greater Accra. It also shows the usefulness of the FR model in flood susceptibility mapping.

### 3.3 Future flood susceptibility projections under the SSP scenarios

Figure 8 compares the flood susceptibility zones in the baseline in 2020 and SSP scenarios in 2055. Likewise the baseline, the coastal and low-lying areas are expected to be more vulnerable to flooding under all SSP scenarios (Fig. 8). However, the FSI differs across scenarios with intensification under the SSP2 and SSP3 (Fig. 8). For instance, Fig. 9 reveals a reduction in the low and moderate flood-susceptible zones under the SSP1 scenario compared to the baseline. The highest area expected to be covered by the moderate flood zone is about 33% under the SSP1 scenario compared to 37% in the baseline period. Also, very low flood- susceptible zones are expected to increase to about 14% of the total area compared to about 7% in the baseline. Generally, flood susceptibility is expected to be moderate under the SSP1 scenario (Fig. 9). However, very high susceptibility zones are expected to slightly increase under the SSP1 scenario compared to the baseline. Between 2020 and 2040 under SSP1, the primary drivers expected to influence flooding occurrence are elevation, slope, distance from urban areas, soil type, and SPI, as detailed in Appendix 1. Notably, by 2045, precipitation replaces SPI as the fifth parameter. Moreover, within the same scenario, precipitation subsequently supplants soil type/geology as the fourth parameter in 2050 and 2055, as indicated in Appendix 1. For the percentage change in flood susceptibility zones, the SSP 1 scenario is expected to observe increase in very low flood susceptibility areas (Fig. 10).

Flood susceptibility projections under the SSP2 scenario reveals similar trends as in SSP1, especially from 2020 to 2035 (see Fig. 10). However, the trend is expected to change from 2040 to 2055. For instance, moderate flood zones are expected to increase to about 41.3% and 43.7% in 2040 and 2045, respectively, compared to about 36.9% in the baseline (Fig. 9). In 2050 and 2055, the percentage of flood susceptibility zones is expected to move from moderate to high zones (about 29.4% and 30.5%, respectively). Again, very high flood susceptibility zones are expected to increase in 2050 (24.3%) and 2055 (25%). As such the SSP2 scenario is expected to observe an increase in high (19.4%) and very high (8.8%) in 2050 as well as an increase of 20.6% in high and very high (9.5%) flood susceptibility zones in 2055 (Fig. 10).

The flood susceptibility projections in the SSP3 scenario resembled those of the SSP2 scenario, showcasing a prevalence of moderate flood susceptibility from 2040 to 2045. Nevertheless, under the SSP3, there's an anticipated rise in

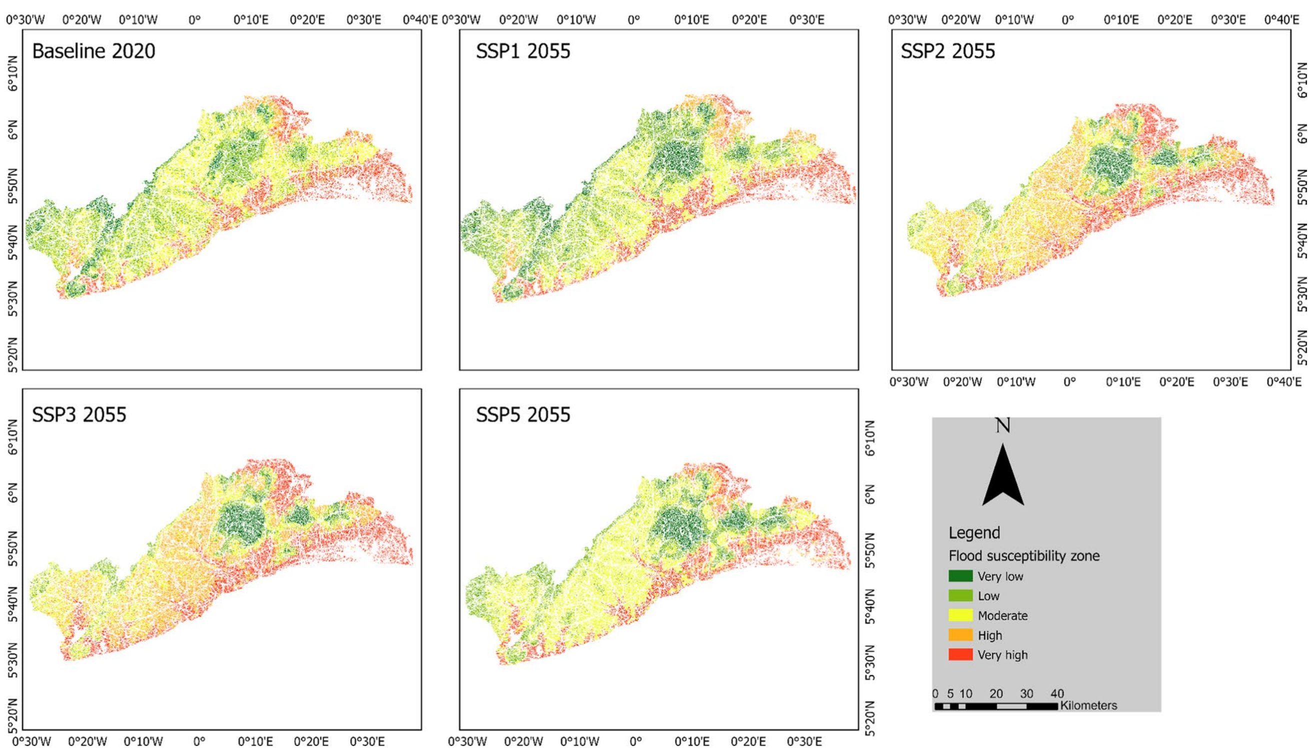


Fig. 8 Flood susceptibility zones under the SSP scenarios in 2055 relative to the baseline

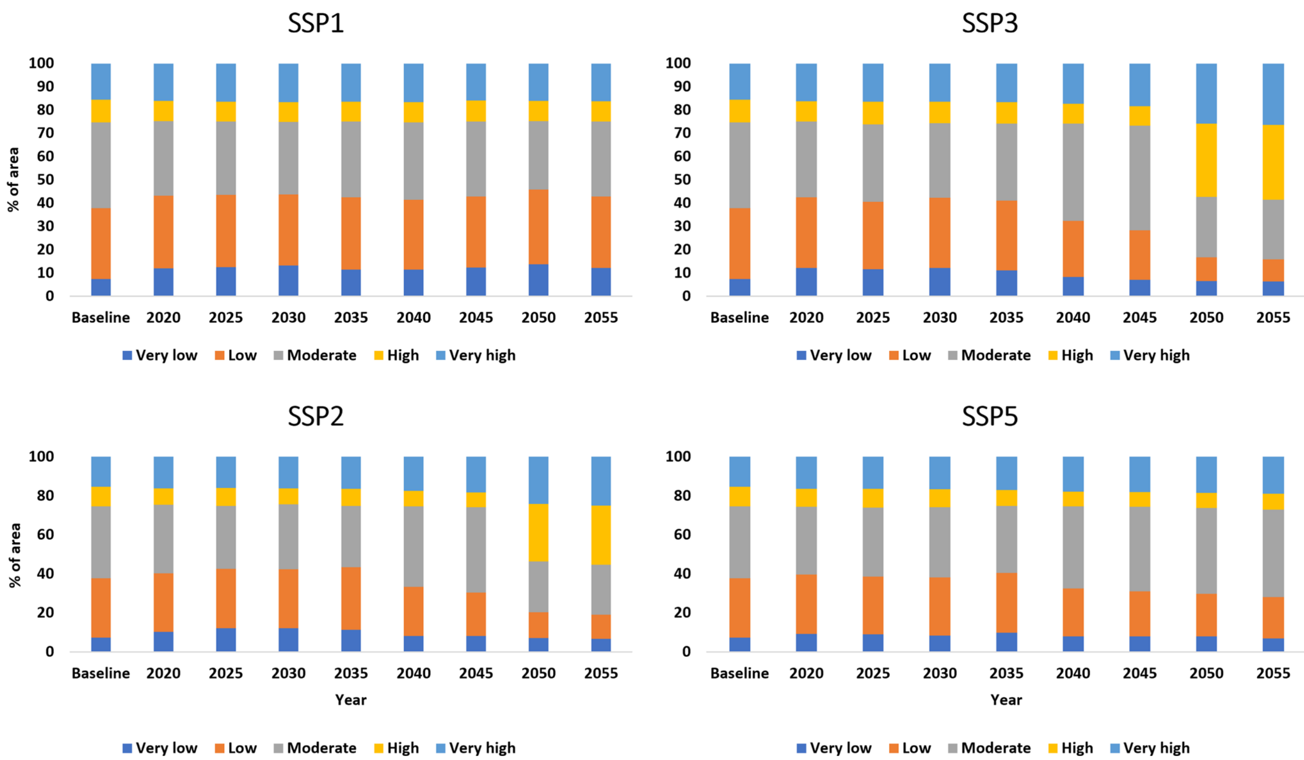


**Fig. 9** Percentage of flood susceptibility zones under the SSP scenarios

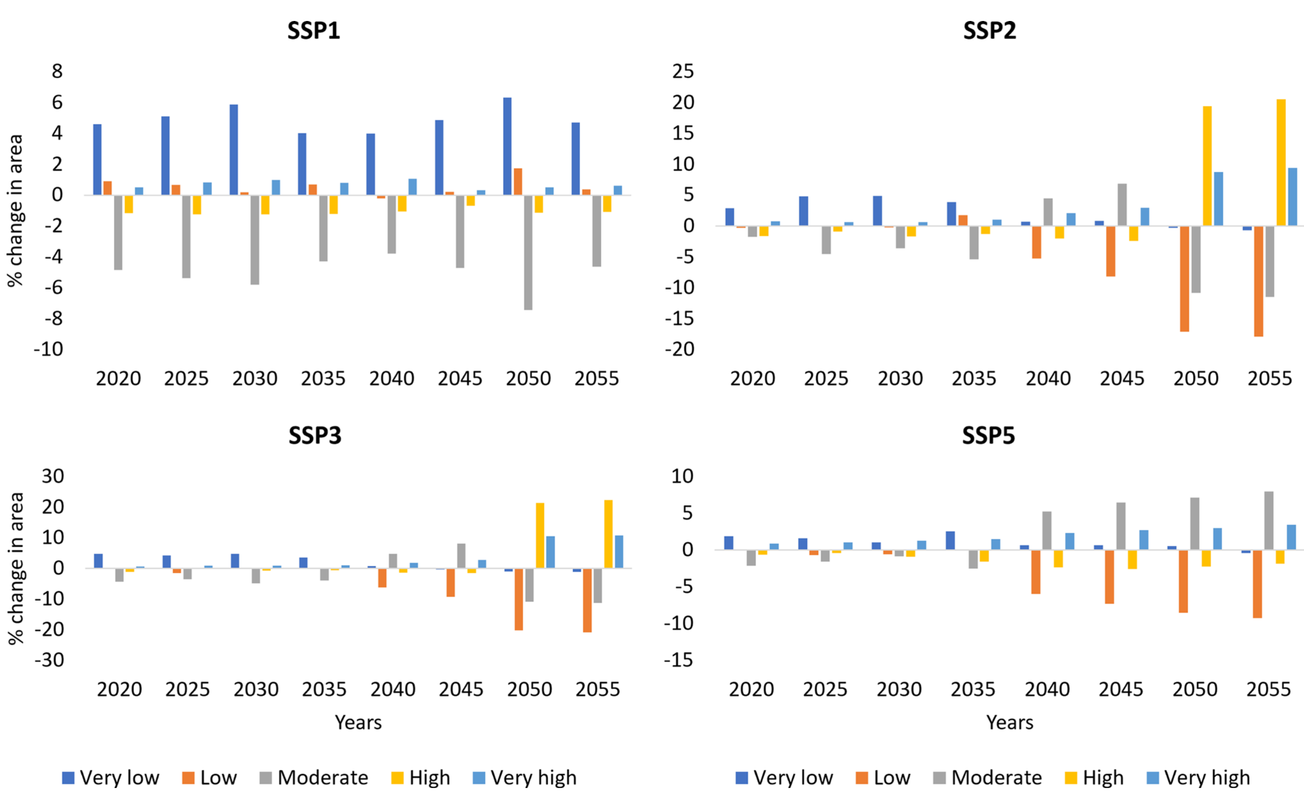


**Fig. 10** Percentage change in flood susceptibility zones under the SSP scenarios relative to the baseline scenario

the extent of high and very high flood susceptibility zones compared to the SSP2. Specifically, the areas categorized as high and very high flood susceptibility zones are projected to expand to approximately 31.4% and 26% respectively by 2050, compared to the respective percentages of 29.4% and 24.3% under SSP2, and are expected to maintain similar increments by 2055 (Fig. 9). This is expected to cause an increase in very high flood susceptibility zones by about 21.5% and 22.3% in 2050 and 2055 respectively.

Elevation, slope, proximity to urban areas, soil type/geology, and SPI are anticipated to serve as the primary influential factors driving flooding occurrences within the SSP2 and SSP3 scenarios, as outlined in Appendix 1. However, the upward movement of distance from urban in the prediction rate, together with other drivers, shifted the dominant flood susceptibility index from moderate to high (see Appendix 1). This is evident in the 2055 of SSP2 and SSP3 where distance from urban became the second most significant flood conditioning factor (see Appendix 1).

For SSP5, flood susceptibility projections reveal a similar trend as SSP1 across all the years under study (see Fig. 10). However, the severity of flood susceptibility differs under the SSP5. Flood susceptibility is generally expected to be in the moderate flood susceptibility zone. However, the moderate flood susceptibility zones are expected to increase especially from 2040 to 2055 (see Fig. 10). For instance, the moderate flood susceptibility zones in 2050 and 2055 are expected to be about 44.41% and 44.47%, respectively, compared to 37% in the baseline year (Fig. 9). The primary influential factors include altitude, incline, proximity to urban areas, soil composition, and rainfall (Appendix 1). The SSP5 scenario is expected to observe increase in moderate and very high flood susceptibility zones especially from 2040 to 2055 (Fig. 10). See Appendix 2 for the spatio-temporal distribution of flood susceptibility zones under the SSPs in Greater Accra.

### 3.4 Flood duration

Figure 11 illustrates a clear trend of increasing flood duration hours in Accra across all modeled rainfall intensity scenarios and future years. Under the moderate flooding scenario, flood duration is projected to rise from a baseline of 320 h per year in 2020 to over 500 h in 2055. The increase is most pronounced in the high rainfall months of March to October. This reflects intensification of precipitation expected under climate change. The high and very high rainfall scenarios, representing more extreme events, show even greater flood duration increases. In the very high scenario, flooding is estimated to reach 640 h in 2045 and exceed 800 h in 2055—more than double the 2020 baseline. While flooding

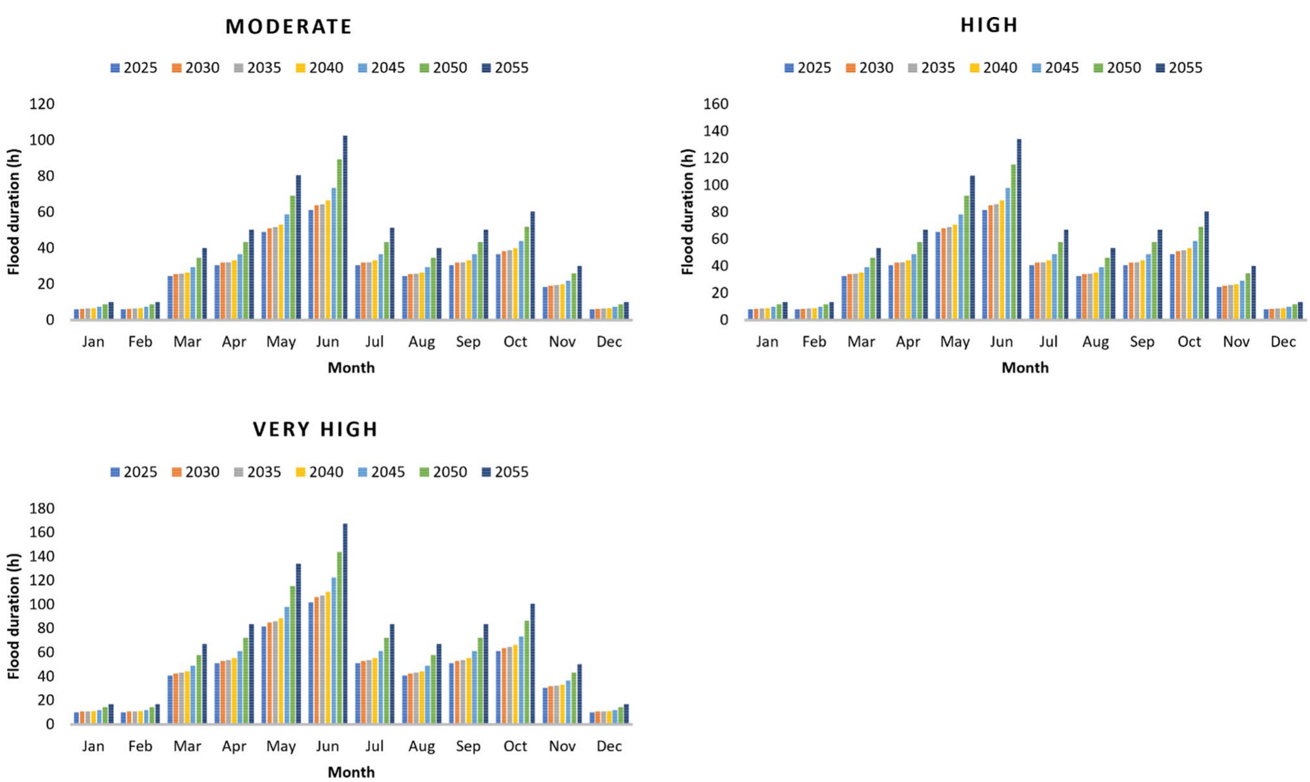


**Fig. 11** Flooding duration for different intensity scenarios

remains higher in the rainy season, the analysis also highlights the risk of extreme rainfall events occurring in typically drier months. December 2055 could see very high rainfall flooding up to 17 h in the month. The results underscore the growing threat seasonal and extreme flooding poses to greater Accra across all rainfall scenarios. Adaptation efforts will need to consider both typical and maximum potential flood levels.

### 3.5 BSP flood risk assessment

The baseline flood susceptibility map in Fig. 12 depicts the locations of bulk supply points, which are labeled with station codes in alphabetical order and their localities. Figure 13 is a chart illustrating the flooding susceptibility of each station under different SSP scenarios. The susceptibility levels range from very low (green) to very high (red). The chart also provides estimates of potential electricity supply curtailed at each station. These estimates are based on the station capacities and duration of flooding and do not consider flood defense systems in the baseline scenario.

The analysis shows the bulk supply points face increasing flood susceptibility, with risks escalating most sharply under the severe climate change SSP3 and SSP5 scenarios. In the 2025–2035 period, over 75% of BSPs fall in the low- to medium-risk categories across SSPs. However, by 2055, more than 50% of BSPs are within medium- to high-risk categories in all scenarios except SSP1, reflecting the impact of climate change. SSP3 and SSP5 stand out with over 60% of BSPs facing high or very high flooding risks by 2055. Coastal and low-lying BSPs like Tema Siemens, Dawhenya, and Awoshie are most vulnerable, with thousands of megawatt-hours denied each year. Persistent failures at these facilities would cripple industrial zones and commercial areas. The results highlight the urgent need for flood resilience adaptation, as power assets currently lack protection. Without major infrastructure improvements, Accra faces severe electricity service disruptions from BSP failures due to flooding, jeopardizing critical facilities and economic functions. Early action under SSP1 to limit emissions and upgrade at-risk BSPs could avoid the worst impacts. However, delayed action under SSP3 and SSP5 could leave Accra's power system highly susceptible to devastating floods. Proactive resilience investments will be essential to ensure BSP operability and energy security for Greater Accra's growing population.

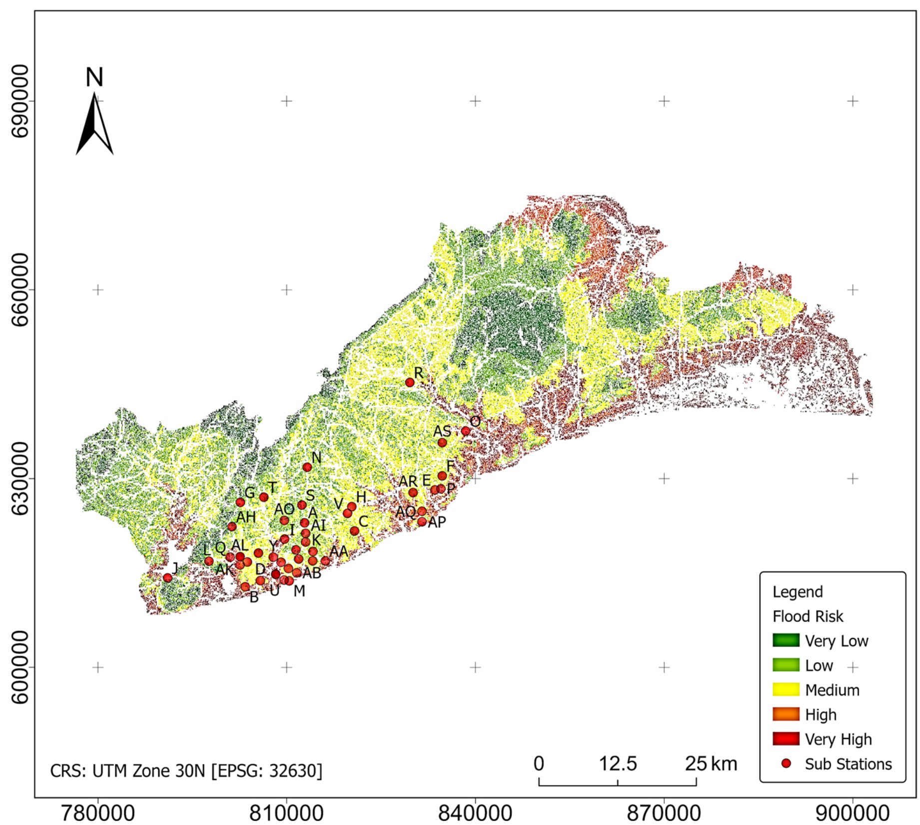


Index of Sub stations

| Name | Location | Alphabet |
|---|---|---|
| Shiashi ECG Substation | Legon | A |
| ECG Sub Station - Exhibition | Dansoman Exhibition | B |
| ECG Substation | Teshie Nungua | C |
| ECG Korle-Bu | Korle Bu | D |
| ECG Substation Tema | Tema Steel Works | E |
| Enclave Power Company substation | Tema | F |
| Electricity Company of Ghana Substation | Ofankor | G |
| GRIDCO ACCRA-EAST SUBSTATION | | H |
| GRIDCO - ACHIMOTA SUBSTATION | Achimota | I |
| E.C.G. Primary Station [Tokose Station Z] | Weija | J |
| ECG Substation, Airport City Substation | Airport | K |
| Gbawe ECG substation | Mallam | L |
| ECG substation 'AH' (Ministries) | Ridge | M |
| ECG Transformer Substation | Adenta | N |
| Dawhenya ECG Sub-Station | Dawhenya | O |
| Seimens Power Plant | Tema | P |
| ECG Power Sub Station | Awoshie | Q |
| AFIENYA BSP | Afienya | R |
| ECG Power Station | Legon | S |
| Station AE | Kwabenya | T |
| Makola station G | Makola | U |
| Station Y Bastona | Spintex, Batsona | V |
| GrIdco accra central | adabraka | W |
| Grqphic road | graphic road | X |
| Avenor | avenor station | Y |
| ECG Station R | Ridge | Z |
| AJ | Tradefair Tseaddo | AA |
| Station X | Osu Kuku hill | AB |
| AU | Cantoments | AC |
| A -ECG substation | Odorkor | AD |
| Station L | Burma Camp | AE |
| ECG substation AS | Kanda substation | AF |
| Station K | Switchback, cantoments | AG |
| ECG station SW | Sowutuom | AH |
| Station AP | Polo grounds | AI |
| Station F | Kokomlemle | AJ |
| ECG substation AW | Awudome | AK |
| ECG substation S | Kwashieman | AL |
| ECG substation AL | Darkuman | AM |
| ECG substation A | Odorkor | AN |
| ECG substation AN | GIMPA | AO |
| Station Q | Tema - Meridian | AP |
| Station A | TdC | AQ |
| Station B | Comm 12 | AR |
| Station C | Comm 25 | AS |

**Fig. 12** 2020 flood susceptibility map of the BSPs

| BSP code | SSP1 (GWh) | | | | | | | SSP2 (GWh) | | | | | | | SSP3 (GWh) | | | | | | | SSP5 (GWh) | | | | | | |
|---|---|---|---|---|---|---|---|---|---|---|---|---|---|---|---|---|---|---|---|---|---|---|---|---|---|---|---|---|
| | 2025 | 2030 | 2035 | 2040 | 2045 | 2050 | 2055 | 2025 | 2030 | 2035 | 2040 | 2045 | 2050 | 2055 | 2025 | 2030 | 2035 | 2040 | 2045 | 2050 | 2055 | 2025 | 2030 | 2035 | 2040 | 2045 | 2050 | 2055 |
| A | 0 | 0 | 0 | 3289 | 3636 | 4283 | 4980 | 3028 | 3152 | 3196 | 3289 | 3636 | 4283 | 6640 | 3028 | 3152 | 3196 | 3289 | 3636 | 5710 | 8300 | 0 | 0 | 0 | 0 | 3636 | 5710 | 4980 |
| B | 0 | 0 | 0 | 3289 | 3636 | 4283 | 4980 | 3028 | 3152 | 3196 | 3289 | 3636 | 4283 | 6640 | 3028 | 3152 | 3196 | 3289 | 3636 | 5710 | 8300 | 3028 | 3152 | 3196 | 3289 | 3636 | 5710 | 4980 |
| C | 0 | 0 | 0 | 3289 | 3636 | 4283 | 4980 | 3028 | 3152 | 3196 | 3289 | 3636 | 4283 | 6640 | 3028 | 3152 | 3196 | 3289 | 3636 | 5710 | 8300 | 3028 | 3152 | 3196 | 3289 | 3636 | 5710 | 6640 |
| D | 0 | 0 | 0 | 3289 | 3636 | 4283 | 4980 | 3028 | 3152 | 3196 | 3289 | 3636 | 4283 | 6640 | 3028 | 3152 | 3196 | 3289 | 4849 | 5710 | 8300 | 3028 | 3152 | 3196 | 3289 | 3636 | 5710 | 6640 |
| E | 0 | 0 | 0 | 0 | 3636 | 4283 | 4980 | 3028 | 3152 | 3196 | 3289 | 3636 | 4283 | 6640 | 3028 | 3152 | 3196 | 3289 | 4849 | 5710 | 8300 | 0 | 0 | 0 | 0 | 3636 | 5710 | 6640 |
| F | 3028 | 3152 | 3196 | 3289 | 3636 | 4283 | 4980 | 3028 | 3152 | 3196 | 3289 | 3636 | 4283 | 6640 | 3028 | 3152 | 3196 | 3289 | 4849 | 5710 | 8300 | 3028 | 3152 | 3196 | 3289 | 3636 | 5710 | 4980 |
| G | 0 | 0 | 0 | 0 | 0 | 0 | 0 | 0 | 0 | 3196 | 3289 | 3636 | 4283 | 4980 | 3028 | 3152 | 3196 | 3289 | 3636 | 4283 | 6640 | 0 | 0 | 0 | 0 | 3636 | 0 | 0 |
| H | 3028 | 3152 | 3196 | 3289 | 3636 | 4283 | 6640 | 3028 | 3152 | 3196 | 3289 | 3636 | 4283 | 6640 | 3028 | 3152 | 3196 | 3289 | 3636 | 5710 | 6640 | 3028 | 3152 | 3196 | 3289 | 3636 | 5710 | 6640 |
| I | 5047 | 5254 | 5327 | 5481 | 6061 | 7138 | 8300 | 5047 | 5254 | 5327 | 5481 | 6061 | 7138 | 8300 | 4038 | 5254 | 5327 | 5481 | 6061 | 7138 | 8300 | 5047 | 5254 | 5327 | 5481 | 6061 | 7138 | 8300 |
| J | 4038 | 4203 | 5327 | 4385 | 6061 | 5710 | 6640 | 4038 | 5254 | 5327 | 5481 | 6061 | 7138 | 8300 | 4038 | 5254 | 5327 | 5481 | 6061 | 7138 | 8300 | 4038 | 5254 | 5327 | 5481 | 6061 | 5710 | 6640 |
| K | 0 | 0 | 0 | 0 | 3636 | 0 | 0 | 0 | 0 | 3196 | 3289 | 3636 | 4283 | 4980 | 0 | 0 | 3196 | 3289 | 3636 | 4283 | 4980 | 0 | 0 | 0 | 0 | 3636 | 0 | 0 |
| L | 3028 | 3152 | 0 | 0 | 0 | 0 | 6640 | 3028 | 3152 | 3196 | 3289 | 3636 | 4283 | 6640 | 3028 | 3152 | 3196 | 3289 | 3636 | 5710 | 8300 | 0 | 3152 | 0 | 0 | 3636 | 0 | 6640 |
| M | 5047 | 5254 | 5327 | 5481 | 6061 | 7138 | 8300 | 5047 | 5254 | 5327 | 5481 | 6061 | 7138 | 8300 | 5047 | 5254 | 5327 | 5481 | 6061 | 7138 | 8300 | 5047 | 5254 | 5327 | 5481 | 6061 | 7138 | 8300 |
| N | 0 | 3152 | 3196 | 3289 | 0 | 4283 | 4980 | 3028 | 0 | 3196 | 3289 | 3636 | 4283 | 4980 | 3028 | 3152 | 3196 | 3289 | 3636 | 4283 | 4980 | 0 | 0 | 0 | 0 | 0 | 4283 | 4980 |
| O | 5047 | 5254 | 5327 | 5481 | 6061 | 7138 | 8300 | 5047 | 5254 | 5327 | 5481 | 6061 | 7138 | 8300 | 5047 | 5254 | 5327 | 5481 | 6061 | 7138 | 8300 | 5047 | 5254 | 5327 | 5481 | 6061 | 7138 | 8300 |
| P | 5047 | 5254 | 5327 | 5481 | 6061 | 7138 | 8300 | 5047 | 5254 | 5327 | 5481 | 6061 | 7138 | 8300 | 5047 | 5254 | 5327 | 5481 | 6061 | 7138 | 8300 | 5047 | 5254 | 5327 | 5481 | 6061 | 7138 | 8300 |
| Q | 5047 | 5254 | 5327 | 5481 | 6061 | 7138 | 8300 | 5047 | 5254 | 5327 | 5481 | 6061 | 7138 | 8300 | 5047 | 5254 | 5327 | 5481 | 6061 | 7138 | 8300 | 5047 | 5254 | 5327 | 5481 | 6061 | 7138 | 8300 |
| R | 0 | 3152 | 0 | 3289 | 3636 | 4283 | 6640 | 3028 | 3152 | 3196 | 3289 | 3636 | 4283 | 6640 | 3028 | 3152 | 3196 | 3289 | 3636 | 5710 | 6640 | 3028 | 3152 | 3196 | 3289 | 3636 | 4283 | 6640 |
| S | 0 | 0 | 0 | 0 | 0 | 0 | 4980 | 0 | 0 | 3196 | 3289 | 3636 | 4283 | 4980 | 0 | 3152 | 3196 | 3289 | 3636 | 4283 | 6640 | 0 | 0 | 0 | 3289 | 0 | 0 | 4980 |
| T | 0 | 0 | 0 | 0 | 0 | 0 | 4980 | 0 | 0 | 3196 | 3289 | 3636 | 4283 | 4980 | 0 | 3152 | 3196 | 3289 | 3636 | 4283 | 6640 | 0 | 0 | 0 | 3289 | 0 | 0 | 4980 |
| U | 4038 | 5254 | 5327 | 5481 | 6061 | 7138 | 8300 | 5047 | 5254 | 4262 | 5481 | 6061 | 7138 | 8300 | 5047 | 5254 | 5327 | 5481 | 6061 | 7138 | 8300 | 5047 | 5254 | 5327 | 5481 | 6061 | 7138 | 8300 |
| V | 3028 | 3152 | 3196 | 3289 | 3636 | 4283 | 6640 | 3028 | 3152 | 3196 | 3289 | 3636 | 4283 | 6640 | 3028 | 3152 | 3196 | 3289 | 3636 | 5710 | 6640 | 3028 | 3152 | 3196 | 3289 | 3636 | 4283 | 6640 |
| W | 5047 | 5254 | 4262 | 5481 | 6061 | 7138 | 8300 | 5047 | 5254 | 5327 | 5481 | 6061 | 7138 | 8300 | 5047 | 5254 | 5327 | 5481 | 6061 | 7138 | 8300 | 5047 | 5254 | 5327 | 5481 | 6061 | 7138 | 8300 |
| X | 5047 | 5254 | 4262 | 5481 | 6061 | 7138 | 8300 | 5047 | 5254 | 5327 | 5481 | 6061 | 7138 | 8300 | 5047 | 5254 | 5327 | 5481 | 6061 | 7138 | 8300 | 5047 | 5254 | 5327 | 5481 | 6061 | 7138 | 8300 |
| Y | 4038 | 4203 | 4262 | 4385 | 6061 | 5710 | 8300 | 4038 | 4203 | 4262 | 5481 | 4849 | 5710 | 8300 | 4038 | 4203 | 4262 | 5481 | 4849 | 7138 | 8300 | 4038 | 4203 | 4262 | 5481 | 6061 | 5710 | 8300 |
| Z | 3028 | 3152 | 3196 | 3289 | 3636 | 4283 | 6640 | 3028 | 3152 | 3196 | 3289 | 3636 | 5710 | 8300 | 3028 | 3152 | 3196 | 3289 | 3636 | 5710 | 6640 | 3028 | 3152 | 3196 | 3289 | 3636 | 4283 | 6640 |
| AA | 5047 | 5254 | 5327 | 5481 | 6061 | 7138 | 8300 | 5047 | 5254 | 5327 | 5481 | 6061 | 7138 | 8300 | 5047 | 5254 | 5327 | 5481 | 6061 | 7138 | 8300 | 5047 | 5254 | 5327 | 5481 | 6061 | 7138 | 8300 |
| AB | 0 | 0 | 0 | 3289 | 3636 | 4283 | 6640 | 3028 | 3152 | 0 | 3289 | 3636 | 4283 | 4980 | 3028 | 3152 | 3196 | 3289 | 3636 | 5710 | 6640 | 3028 | 3152 | 3196 | 3289 | 3636 | 4283 | 6640 |
| AC | 3028 | 3152 | 3196 | 3289 | 3636 | 4283 | 6640 | 3028 | 3152 | 3196 | 3289 | 3636 | 4283 | 6640 | 3028 | 3152 | 3196 | 3289 | 3636 | 5710 | 6640 | 3028 | 3152 | 3196 | 3289 | 3636 | 4283 | 6640 |
| AD | 3028 | 3152 | 3196 | 3289 | 3636 | 4283 | 6640 | 3028 | 3152 | 3196 | 3289 | 3636 | 4283 | 6640 | 3028 | 3152 | 3196 | 3289 | 3636 | 5710 | 6640 | 3028 | 3152 | 3196 | 3289 | 3636 | 4283 | 6640 |
| AE | 3028 | 3152 | 3196 | 3289 | 3636 | 4283 | 6640 | 0 | 3152 | 0 | 3289 | 3636 | 4283 | 6640 | 3028 | 3152 | 3196 | 3289 | 3636 | 5710 | 6640 | 3028 | 3152 | 3196 | 3289 | 3636 | 4283 | 6640 |
| AF | 3028 | 0 | 3196 | 3289 | 3636 | 0 | 4980 | 0 | 0 | 0 | 3289 | 3636 | 4283 | 6640 | 3028 | 0 | 0 | 3289 | 0 | 4283 | 4980 | 0 | 0 | 0 | 3289 | 3636 | 0 | 4980 |
| AG | 3028 | 3152 | 3196 | 3289 | 3636 | 4283 | 6640 | 3028 | 3152 | 3196 | 3289 | 3636 | 5710 | 8300 | 3028 | 3152 | 3196 | 3289 | 3636 | 5710 | 6640 | 3028 | 3152 | 3196 | 3289 | 3636 | 4283 | 6640 |
| AH | 0 | 0 | 0 | 0 | 0 | 0 | 4980 | 0 | 0 | 0 | 0 | 0 | 0 | 4980 | 0 | 0 | 0 | 3289 | 3636 | 4283 | 4980 | 0 | 0 | 0 | 0 | 0 | 0 | 4980 |
| AI | 3028 | 3152 | 3196 | 3289 | 3636 | 4283 | 4980 | 0 | 3152 | 3196 | 3289 | 3636 | 5710 | 6640 | 3028 | 3152 | 0 | 3289 | 4849 | 5710 | 6640 | 3028 | 3152 | 3196 | 3289 | 3636 | 4283 | 4980 |
| AJ | 5047 | 5254 | 5327 | 5481 | 6061 | 7138 | 8300 | 5047 | 5254 | 5327 | 5481 | 6061 | 7138 | 8300 | 5047 | 5254 | 5327 | 5481 | 6061 | 7138 | 8300 | 5047 | 5254 | 5327 | 5481 | 6061 | 7138 | 8300 |
| AK | 3028 | 3152 | 3196 | 3289 | 3636 | 4283 | 6640 | 3028 | 3152 | 0 | 3289 | 3636 | 4283 | 6640 | 3028 | 3152 | 3196 | 3289 | 3636 | 5710 | 6640 | 3028 | 3152 | 3196 | 3289 | 3636 | 4283 | 6640 |
| AL | 3028 | 3152 | 3196 | 3289 | 3636 | 4283 | 6640 | 3028 | 3152 | 0 | 3289 | 3636 | 4283 | 6640 | 3028 | 3152 | 3196 | 3289 | 3636 | 5710 | 6640 | 3028 | 3152 | 3196 | 3289 | 3636 | 4283 | 6640 |
| AM | 0 | 0 | 0 | 0 | 3636 | 0 | 6640 | 0 | 0 | 0 | 3289 | 3636 | 4283 | 6640 | 0 | 0 | 0 | 3289 | 3636 | 4283 | 4980 | 0 | 0 | 0 | 3289 | 3636 | 0 | 6640 |
| AN | 3028 | 3152 | 3196 | 3289 | 3636 | 4283 | 6640 | 3028 | 3152 | 0 | 3289 | 3636 | 5710 | 6640 | 3028 | 3152 | 3196 | 3289 | 3636 | 5710 | 6640 | 3028 | 3152 | 3196 | 3289 | 3636 | 4283 | 6640 |
| AO | 3028 | 3152 | 3196 | 3289 | 3636 | 4283 | 6640 | 3028 | 3152 | 0 | 3289 | 3636 | 5710 | 6640 | 3028 | 3152 | 3196 | 3289 | 3636 | 4283 | 6640 | 3028 | 3152 | 3196 | 3289 | 3636 | 4283 | 6640 |
| AP | 0 | 0 | 0 | 0 | 3636 | 5710 | 6640 | 3028 | 3152 | 3196 | 3289 | 3636 | 5710 | 6640 | 5047 | 4203 | 4262 | 4385 | 4849 | 5710 | 6640 | 0 | 4203 | 4262 | 4385 | 3636 | 5710 | 6640 |
| AQ | 3028 | 3152 | 0 | 0 | 3636 | 4283 | 4980 | 3028 | 3152 | 3196 | 3289 | 3636 | 5710 | 6640 | 3028 | 0 | 0 | 3289 | 3636 | 5710 | 6640 | 3028 | 0 | 0 | 3289 | 3636 | 4283 | 4980 |
| AR | 3028 | 3152 | 3196 | 3289 | 3636 | 4283 | 4980 | 3028 | 3152 | 3196 | 3289 | 3636 | 5710 | 6640 | 3028 | 3152 | 3196 | 3289 | 3636 | 5710 | 6640 | 3028 | 3152 | 3196 | 3289 | 3636 | 4283 | 4980 |
| AS | 3028 | 3152 | 3196 | 0 | 3636 | 4283 | 4980 | 3028 | 3152 | 3196 | 3289 | 3636 | 5710 | 6640 | 3028 | 3152 | 3196 | 3289 | 3636 | 5710 | 6640 | 0 | 0 | 0 | 3289 | 3636 | 4283 | 4980 |

**Fig. 13** BSP flood susceptibilities and power denied across SSP scenarios

### 3.6 Power curtailed due to flooding

The flood risk analysis shows power denied due to outages escalating over time, but with distinct trends across scenarios as shown in Fig. 14. SSP1 sees the smallest increases, rising from 112 GWh in 2025 to 279 GWh in 2055—a 4.2% of the total electricity supply of 3685.77 GWh annually for the BSPs considered. SSP2 and SSP3 follow similar growth trajectories, reaching over 300 GWh and 5% supply loss by 2055. However, SSP5 denial remains the second lowest, peaking at 284 GWh (4.4%) in 2055. The results indicate that persistent losses of this magnitude would require load shedding and blackouts during major flood events. Even SSP1, the best case climate change and socioeconomic development scenario, could see significant local outages from flooded BSPs. There is the need to target adaptation investments at vulnerable BSPs. Protecting or relocating a few high-risk facilities could maintain electricity access for most customers, even if flooding increases.

## 4 Discussion

### 4.1 Flood projections under the SSP scenarios in the Greater Accra region

The results of the study show high positive correlation between the flood conditioning factors and the occurrence of flooding in the Greater Accra region as revealed by the FR values. Elevation, distance from urban, slope, soil, SPI and precipitation were the first five most sensitive parameters that is expected to influence flooding in the

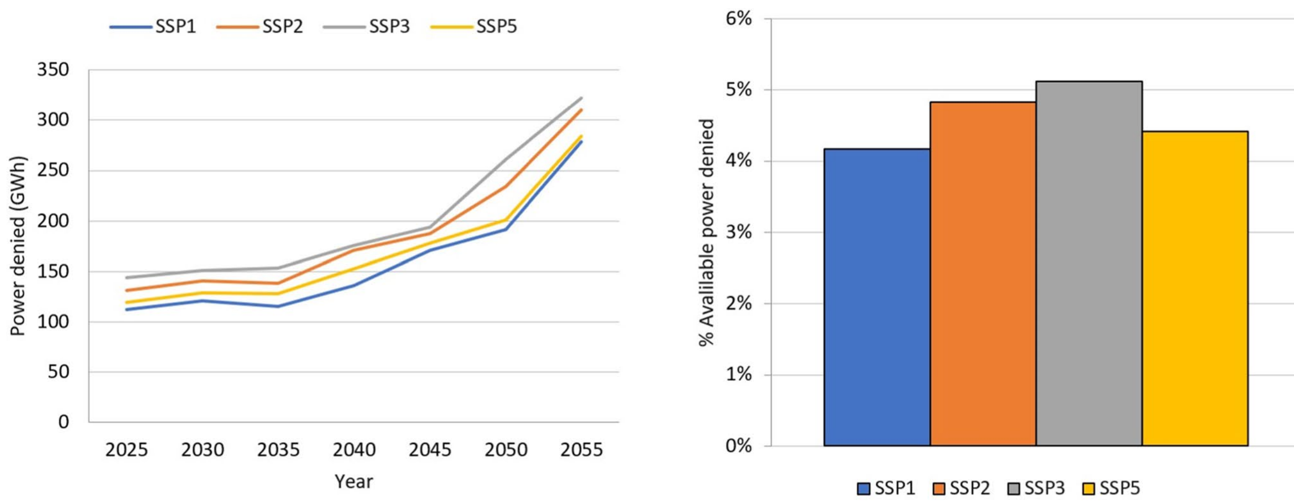


**Fig. 14** Electricity denied forecast (left) and percentage of electricity denied from total BSP supply (right)

Greater Accra region, with SPI and precipitation interchanging positions under the SSP scenarios. Several studies have attributed flooding in Greater Accra to non-meteorological factors [70]. For instance, elevation was generally found to be the most sensitive flood condition factor in the Greater Accra region as areas between 21 and 47.25 m above sea level (especially areas along the coastal line) were found to be highly vulnerable in the historical and future periods. The study of Ansah et al. [70] revealed that Accra is a coastal region at low altitude that receives run-offs from high altitude, especially in the month of June, which is the peak of the major rainy season over southern Ghana. Consecutive wet days over inland areas and high grounds continually drained off to the sea. Due to the low-lying nature of the Greater Accra region, the run-offs accumulate, resulting in stray waters entering urban and unprotected areas. While elevation may not fall under meteorological flood conditioning factors, it remains a significant natural element in flood occurrence. Given the challenging nature of addressing natural factors, adaptation strategies need to carefully account for additional factors, such as proximity to urban areas, for effective flood management in the region.

Again, distance from urban areas is the second-most sensitive flood conditioning factor in the Greater Accra region, especially in the future under the SSP scenarios. The SSP2 and SSP3 scenarios are expected to be the worst-case scenarios where high flood susceptibility zones are expected to generally dominate. This may be attributed to the population projections under the SSP2 and SSP3 scenarios. For instance, population is expected to hit 9 and 12.6 billion by the end of the twenty-first century [72]. These increases are expected to affect urban growth since population and urbanization have a proportional relationship. Therefore, as population increases, urbanization is expected to also increase, which provides conditions conducive to flooding, especially in an already densely populated region like in Greater Accra. As a result, distance from urban was found to have great influence on the occurrence of flooding in the Greater Accra region, especially from 2040 to 2055 under SSP2 and SSP3. The proliferation of hardscapes, unplanned settlements in flood-prone areas, poor drainage systems, limited tree planting, limited roof-top rain harvesting systems, and unplanned settlements and settlements in riparian zones and wetlands, coupled with the high generation of solid waste which ends up in drains other areas are associated with urban sprawl, which leads to increased run-off in these areas [1, 19, 70, 73]. As a result, even moderate precipitation can trigger floods, posing a significant challenge for city planners, particularly regarding the management of infrastructural development in the area [70]. The sensitivity of the flood conditioning factors, such as slope, soil type and SPI, persisted consistently across all the SSP scenarios in the Greater Accra region. However, precipitation as a meteorological flood conditioning factor was amongst the top flood conditioning factors under the SSP1 and SSP5 scenarios. Soil type or geology was identified as one of the most influential factors contributing to flood occurrence in the region. Studies indicated that areas within the Accra metropolis characterized by Accranian and Togo series rock types experienced more frequent high floods. Geological formations prevalent in the Dahomeyan series were observed to channel runoff toward low-lying areas, thereby exacerbating flooding in the region, particularly within the Accra metropolis [45].

### 4.2 Flood resilience measures

The results show Accra's power system should increase adaptation measures to manage future supply impacts due to flooding as persistent flooding of these facilities would paralyze southern Accra's power supply chain. Key industrial and commercial areas could face prolonged blackouts during flood events, and hospitals, water services, and other critical infrastructure would be jeopardized.

To enhance resilience, flood defenses should be prioritized at the most vulnerable BSPs, like Achimota, Weija, Ridge, Dawhenya, Tema, Awoshie, Afienya, Spintex, Adabraka, Avenor, Tseaddo, Kokomlemle, and and Graphic Road substations. Elevating or relocating flood-prone components like transformers could enable them to function during lower-level flooding events [74]. Construction of berms, floodwalls, and raised access roads would shield facilities from extreme flooding. This approach has been explored in the context of flood prevention devices for transformer substations, where a baffle made of metal material is used to control floodwaters and prevent them from entering the substation [75]. Additionally, the concept of flexible transformers has been proposed, which can be used as replacements for different voltage levels and have adjustable impedance features to match the requirements of impacted substations [76, 77]. These flexible transformers have been proven to be functional and stable in both factory lab and field tests [78]. Furthermore, the use of flood monitoring systems with float switches which allows operators to de-energize equipment or substations prior to loss of control and eventual damage can be used as an early warning system [75]. In constructing new BSPs in high-risk zones should be avoided. Where relocation is infeasible, redundant connections and distributed supply sources, such as solar photovoltaic power with battery storage, could maintain power when legacy assets are flooded. Corrosion-resistant or galvanized substation equipment, such as bracing, purlins, and exterior panels can also be used where relocation is impractical [79]. By implementing these strategies, the impact of flooding on transformer substations can be reduced, ensuring a more reliable energy supply.

## 5 Conclusion

This study analyzed current and future flood risks and their impacts on electricity bulk supply points in Greater Accra, Ghana under different climate change (Shared Socioeconomic Pathway) scenarios. The study used 16 flood conditioning factors in simulating current and future flood conditions under the SSP scenarios using the Frequency Ratio (FR) model. The performance of the model was evaluated using the Receiver Operating Characteristic (ROC) curve, displaying high accuracy (an Area under the curve (AUC) value of 0.83) for flood susceptibility mapping in Greater Accra. Analysis reveals elevation, distance from urban areas, slope, soil type, SPI, and precipitation as the primary influential parameters increasing flood susceptibility in the region. Notably, elevation emerges as a critical factor, especially for areas near the coast between 21 and 47.25 m above sea level. Moreover, the distance from urban areas, particularly under SSP2 and SSP3 scenarios, emerges as another significant factor affecting flooding due to population growth and subsequent urbanization. Moreover, the study identified vulnerable electricity infrastructure and projected potential impacts on power supply for the region under the SSP scenarios. The results illustrate the urgent need to adapt Accra's power system infrastructure to increasing flood hazards driven by climate change. Electricity disruption due to flooding is projected to grow, leaving coastal and low-lying bulk supply points at high risk. Persistent flooding of these facilities would cripple Accra's electricity supply chain, jeopardizing key services and economic functions. To enhance resilience, the study recommends prioritizing upgrades like flood barriers, elevated equipment, and infrastructure hardening at the highest-risk bulk supply points. Restricting new development in floodplains is also critical to limit exposure. Collaborative adaptation efforts between utilities, government agencies, and communities will be essential to develop tailored resilience strategies. Model coupling with long-term energy system optimization models will also reveal optimal energy planning pathways to mitigate flooding impacts in the future, as part of further studies.

**Acknowledgements** This study was supported by the Swiss National Science Foundation (SNF) (grant number IZSTZ0_193649). The authors are grateful for the support. The authors also thank the Regional Center for Energy and Environmental Sustainability at the University of Energy and Natural Resources for their support.

**Author contributions** E.K.S.: Writing – review & editing, Writing – original draft, Validation, Resources, Investigation, Data curation, Formal analysis. A.A.P.: Formal analysis, Data curation, Writing – review & editing, Writing – original draft. N.O.O.: Writing – review & editing, Writing – original draft. E.A.A.: Writing – review & editing, Supervision. A.T.K.: Writing – review & editing, Supervision. N.S.A.D.: Writing – review & editing, Supervision. K.A.: Writing – review & editing, Supervision. G.K.A.: Writing – review & editing, Supervision. E.A.A.: Writing – review & editing. F.K.: Writing – review & editing, Supervision. M.Y.: Supervision, Writing – review & editing, Writing – original draft.

**Funding** This study was supported by the Swiss National Science Foundation (SNF) (grant number IZSTZ0_193649). The authors are grateful for the support.

**Data availability** The flood risk maps that supports findings of this study have been deposited in Zenodo with DOI: https://zenodo.org/doi/https://doi.org/10.5281/zenodo.10631311.

## Declarations

**Competing interests** The authors declare no competing interests.



## Appendix 1: Prediction rates of flood conditioning factors

| 2020 | | 2025 | | 2030 | | 2035 | | 2040 | | 2045 | | 2050 | | 2055 | |
|---|---|---|---|---|---|---|---|---|---|---|---|---|---|---|---|
| Factors | Prediction rate | Factors | Prediction rate | Factors | Prediction rate | Factors | Prediction rate | Factors | Prediction rate | Factors | Prediction rate | Factors | Prediction rate | Factors | Prediction rate |
| SSP1 | | | | | | | | | | | | | | | |
| 1 | 1.000 | 1 | 1.000 | 1 | 1.000 | 1 | 1.000 | 1 | 1.000 | 1 | 1.000 | 1 | 1.000 | 1 | 1.000 |
| 2 | 3.975 | 2 | 3.975 | 2 | 3.975 | 2 | 3.975 | 2 | 3.975 | 2 | 3.975 | 2 | 3.975 | 2 | 3.975 |
| 3 | 9.158 | 3 | 9.158 | 3 | 9.158 | 3 | 9.158 | 3 | 9.158 | 3 | 9.158 | 3 | 9.158 | 3 | 9.158 |
| 4 | 11.211 | 4 | 11.211 | 4 | 11.211 | 4 | 11.211 | 4 | 11.211 | 4 | 11.211 | 4 | 11.211 | 4 | 11.211 |
| 5 | 11.355 | 5 | 11.355 | 5 | 11.355 | 5 | 11.355 | 5 | 11.355 | 5 | 11.355 | 5 | 11.355 | 5 | 11.355 |
| 6 | 18.283 | 7 | 19.773 | 7 | 19.738 | 6 | 18.676 | 7 | 19.171 | 7 | 17.743 | 7 | 16.668 | 7 | 15.487 |
| 7 | 19.630 | 6 | 19.988 | 8 | 21.024 | 7 | 20.168 | 6 | 20.773 | 8 | 21.024 | 8 | 21.024 | 8 | 21.024 |
| 8 | 21.024 | 8 | 21.024 | 6 | 22.291 | 8 | 21.024 | 8 | 21.024 | 9 | 22.674 | 9 | 22.674 | 9 | 22.674 |
| 9 | 22.674 | 9 | 22.674 | 9 | 22.674 | 9 | 22.674 | 9 | 22.674 | 10 | 24.830 | 10 | 24.830 | 10 | 24.830 |
| 10 | 24.830 | 10 | 24.830 | 10 | 24.830 | 10 | 24.830 | 10 | 24.830 | 11 | 27.108 | 11 | 27.108 | 11 | 27.108 |
| 11 | 27.108 | 11 | 27.108 | 11 | 27.108 | 11 | 27.108 | 11 | 27.108 | 6 | 29.182 | 12 | 29.552 | 12 | 29.552 |
| 12 | 29.552 | 12 | 29.552 | 12 | 29.552 | 12 | 29.552 | 12 | 29.552 | 12 | 29.552 | 6 | 36.855 | 6 | 35.850 |
| 13 | 37.987 | 13 | 38.021 | 13 | 38.058 | 13 | 38.469 | 13 | 38.919 | 13 | 39.768 | 13 | 40.526 | 13 | 41.185 |
| 14 | 43.760 | 14 | 43.760 | 14 | 43.760 | 14 | 43.760 | 14 | 43.760 | 14 | 43.760 | 14 | 43.760 | 14 | 43.760 |
| 15 | 69.800 | 15 | 69.800 | 15 | 69.800 | 15 | 69.800 | 15 | 69.800 | 15 | 69.800 | 15 | 69.800 | 15 | 69.800 |
| SSP2 | | | | | | | | | | | | | | | |
| 1 | 1.000 | 1 | 1.000 | 1 | 1.000 | 1 | 1.000 | 1 | 1.000 | 1 | 1.000 | 1 | 1.000 | 1 | 1.000 |
| 2 | 3.975 | 2 | 3.975 | 2 | 3.975 | 2 | 3.975 | 2 | 3.975 | 2 | 3.975 | 2 | 3.975 | 2 | 3.975 |
| 3 | 9.158 | 3 | 9.158 | 3 | 9.158 | 3 | 9.158 | 3 | 9.158 | 3 | 9.158 | 3 | 9.158 | 3 | 9.158 |
| 4 | 11.211 | 4 | 11.211 | 4 | 11.211 | 4 | 11.211 | 4 | 11.211 | 4 | 11.211 | 4 | 11.211 | 4 | 11.211 |
| 5 | 11.355 | 5 | 11.355 | 5 | 11.355 | 5 | 11.355 | 5 | 11.355 | 5 | 11.355 | 5 | 11.355 | 5 | 11.355 |
| 6 | 18.794 | 7 | 19.665 | 6 | 18.168 | 7 | 18.574 | 6 | 15.515 | 7 | 16.058 | 7 | 14.308 | 7 | 13.239 |
| 7 | 21.024 | 8 | 21.024 | 7 | 18.795 | 6 | 20.518 | 7 | 17.508 | 6 | 20.816 | 6 | 17.041 | 6 | 21.001 |
| 8 | 22.674 | 9 | 22.674 | 8 | 21.024 | 8 | 21.024 | 8 | 21.024 | 8 | 21.024 | 8 | 21.024 | 8 | 21.024 |
| 9 | 24.047 | 6 | 23.138 | 9 | 22.674 | 9 | 22.674 | 9 | 22.674 | 9 | 22.674 | 9 | 22.674 | 9 | 22.674 |

| 2020 | | 2025 | | 2030 | | 2035 | | 2040 | | 2045 | | 2050 | | 2055 | |
|---|---|---|---|---|---|---|---|---|---|---|---|---|---|---|---|
| Factors | Prediction rate | Factors | Prediction rate | Factors | Prediction rate | Factors | Prediction rate | Factors | Prediction rate | Factors | Prediction rate | Factors | Prediction rate | Factors | Prediction rate |
| 10 | 24.830 | 10 | 24.830 | 10 | 24.830 | 10 | 24.830 | 10 | 24.830 | 10 | 24.830 | 10 | 24.830 | 10 | 24.830 |
| 11 | 27.108 | 11 | 27.108 | 11 | 27.108 | 11 | 27.108 | 11 | 27.108 | 11 | 27.108 | 11 | 27.108 | 11 | 27.108 |
| 12 | 29.552 | 12 | 29.552 | 12 | 29.552 | 12 | 29.552 | 12 | 29.552 | 12 | 29.552 | 12 | 29.552 | 12 | 29.552 |
| 13 | 38.435 | 13 | 38.010 | 13 | 38.320 | 13 | 39.111 | 13 | 40.049 | 13 | 41.221 | 13 | 43.052 | 13 | 43.760 |
| 14 | 43.760 | 14 | 43.760 | 14 | 43.760 | 14 | 43.760 | 14 | 43.760 | 14 | 43.760 | 14 | 43.760 | 14 | 44.714 |
| 15 | 69.800 | 15 | 69.800 | 15 | 69.800 | 15 | 69.800 | 15 | 69.800 | 15 | 69.800 | 15 | 69.800 | 15 | 69.800 |
| SSP3 | | | | | | | | | | | | | | | |
| 1 | 1.000 | 1 | 1.000 | 1 | 1.000 | 1 | 1.000 | 1 | 1.000 | 1 | 1.000 | 1 | 1.000 | 1 | 1.000 |
| 2 | 3.975 | 2 | 3.975 | 2 | 3.975 | 2 | 3.975 | 2 | 3.975 | 2 | 3.975 | 2 | 3.975 | 2 | 3.975 |
| 3 | 9.158 | 3 | 9.158 | 3 | 9.158 | 3 | 9.158 | 3 | 9.158 | 3 | 9.158 | 3 | 9.158 | 3 | 9.158 |
| 4 | 11.211 | 4 | 11.211 | 4 | 11.211 | 4 | 11.211 | 4 | 11.211 | 4 | 11.211 | 4 | 11.211 | 4 | 11.211 |
| 5 | 11.355 | 5 | 11.355 | 5 | 11.355 | 5 | 11.355 | 5 | 11.355 | 5 | 11.355 | 5 | 11.355 | 5 | 11.355 |
| 6 | 18.536 | 7 | 19.722 | 6 | 15.515 | 7 | 19.029 | 7 | 16.786 | 7 | 17.312 | 7 | 14.104 | 7 | 12.966 |
| 7 | 18.813 | 8 | 21.024 | 7 | 19.728 | 8 | 21.024 | 6 | 17.646 | 8 | 21.024 | 8 | 21.024 | 8 | 21.024 |
| 8 | 21.024 | 6 | 21.845 | 8 | 21.024 | 9 | 22.674 | 8 | 21.024 | 9 | 22.674 | 9 | 22.674 | 6 | 21.936 |
| 9 | 22.674 | 9 | 22.674 | 9 | 22.674 | 6 | 24.668 | 9 | 22.674 | 10 | 24.830 | 6 | 22.995 | 9 | 22.674 |
| 10 | 24.830 | 10 | 24.830 | 10 | 24.830 | 10 | 24.830 | 10 | 24.830 | 6 | 25.926 | 10 | 24.830 | 10 | 24.830 |
| 11 | 27.108 | 11 | 27.108 | 11 | 27.108 | 11 | 27.108 | 11 | 27.108 | 11 | 27.108 | 11 | 27.108 | 11 | 27.108 |
| 12 | 29.552 | 12 | 29.552 | 12 | 29.552 | 12 | 29.552 | 12 | 29.552 | 12 | 29.552 | 12 | 29.552 | 12 | 29.552 |
| 13 | 38.964 | 13 | 38.004 | 13 | 37.966 | 13 | 38.518 | 13 | 39.128 | 13 | 40.026 | 13 | 42.983 | 14 | 43.760 |
| 14 | 43.760 | 14 | 43.760 | 14 | 43.760 | 14 | 43.760 | 14 | 43.760 | 14 | 43.760 | 14 | 43.760 | 13 | 44.552 |
| 15 | 69.800 | 15 | 69.800 | 15 | 69.800 | 15 | 69.800 | 15 | 69.800 | 15 | 69.800 | 15 | 69.800 | 15 | 69.800 |
| SSP5 | | | | | | | | | | | | | | | |
| 1 | 1.000 | 1 | 1.000 | 1 | 1.000 | 1 | 1.000 | 1 | 1.000 | 1 | 1.000 | 1 | 1.000 | 1 | 1.000 |
| 2 | 3.975 | 2 | 3.975 | 2 | 3.975 | 2 | 3.975 | 2 | 3.975 | 2 | 3.975 | 2 | 3.975 | 2 | 3.975 |
| 3 | 9.158 | 3 | 9.158 | 3 | 9.158 | 3 | 9.158 | 3 | 9.158 | 3 | 9.158 | 3 | 9.158 | 3 | 9.158 |
| 4 | 11.211 | 4 | 11.211 | 4 | 11.211 | 4 | 11.211 | 4 | 11.211 | 4 | 11.211 | 4 | 11.211 | 4 | 11.211 |
| 5 | 11.355 | 5 | 11.355 | 5 | 11.355 | 5 | 11.355 | 5 | 11.355 | 5 | 11.355 | 5 | 11.355 | 5 | 11.355 |
| 6 | 17.586 | 7 | 19.610 | 7 | 19.526 | 7 | 18.812 | 7 | 18.649 | 7 | 17.427 | 7 | 16.597 | 7 | 15.631 |
| 7 | 17.816 | 8 | 21.024 | 8 | 21.024 | 8 | 21.024 | 8 | 21.024 | 8 | 21.024 | 8 | 21.024 | 8 | 21.024 |
| 8 | 21.024 | 9 | 22.674 | 9 | 22.674 | 9 | 22.674 | 9 | 22.674 | 9 | 22.674 | 6 | 21.485 | 9 | 22.674 |
| 9 | 22.674 | 10 | 24.830 | 10 | 24.830 | 10 | 24.830 | 10 | 24.830 | 10 | 24.830 | 9 | 22.674 | 6 | 24.654 |
| 10 | 24.830 | 11 | 27.108 | 11 | 27.108 | 11 | 27.108 | 11 | 27.108 | 11 | 27.108 | 10 | 24.830 | 10 | 24.830 |
| 11 | 27.108 | 6 | 27.957 | 12 | 29.552 | 12 | 29.552 | 6 | 29.273 | 6 | 28.728 | 11 | 27.108 | 11 | 27.108 |
| 12 | 29.552 | 12 | 29.552 | 6 | 36.438 | 6 | 32.997 | 12 | 29.552 | 12 | 29.552 | 12 | 29.552 | 12 | 29.552 |
| 13 | 39.810 | 13 | 38.019 | 13 | 38.083 | 13 | 38.513 | 13 | 38.957 | 13 | 39.812 | 13 | 40.554 | 13 | 41.294 |
| 14 | 43.760 | 14 | 43.760 | 14 | 43.760 | 14 | 43.760 | 14 | 43.760 | 14 | 43.760 | 14 | 43.760 | 14 | 43.760 |
| 15 | 69.800 | 15 | 69.800 | 15 | 69.800 | 15 | 69.800 | 15 | 69.800 | 15 | 69.800 | 15 | 69.800 | 15 | 69.800 |

Factors: Curvature = 1, Aspect = 2, Drainage density = 3, TWI = 4, Distance from stream = 5, Precipitation for the respective year = 6, LULC for the respective year = 7, STI = 8, NDVI = 9, Distance to road = 10, SPI = 11, soil/geology = 12, Distance from urban for the respective year = 13, slope = 14, Elevation = 15.

## Appendix 2: Flood vulnerability maps

See Figs. 15, 16, 17 and 18.

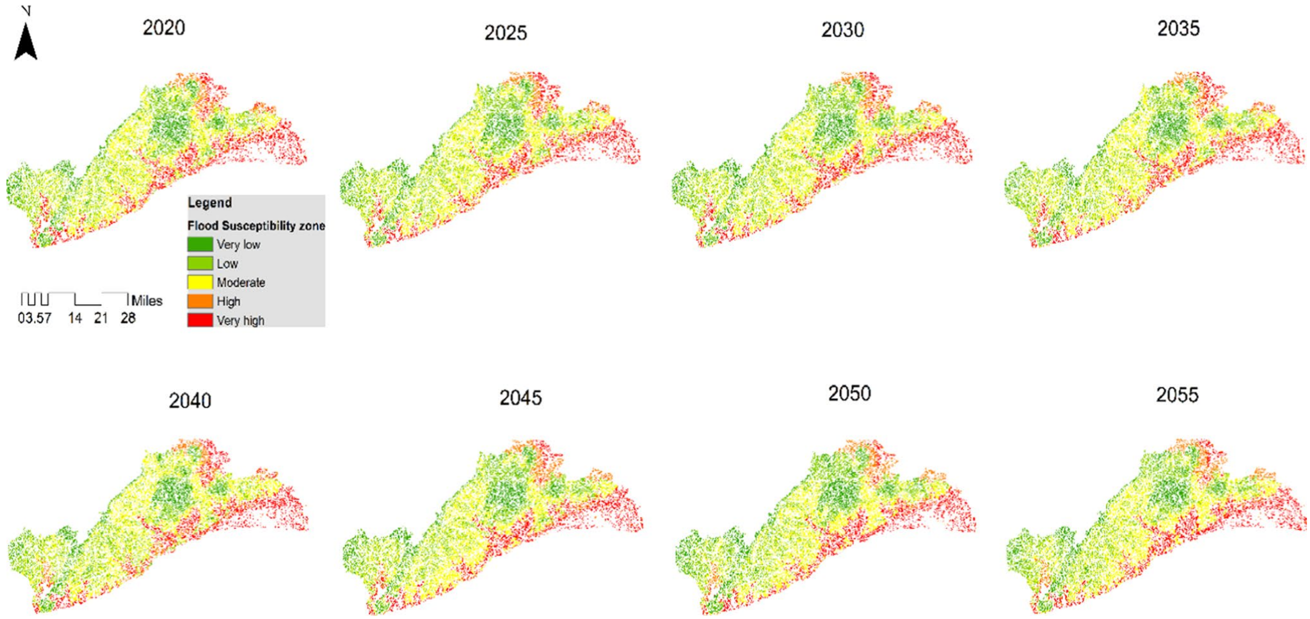


**Fig. 15** Spatio-temporal distribution of flood vulnerability zones under the SSP1 scenario

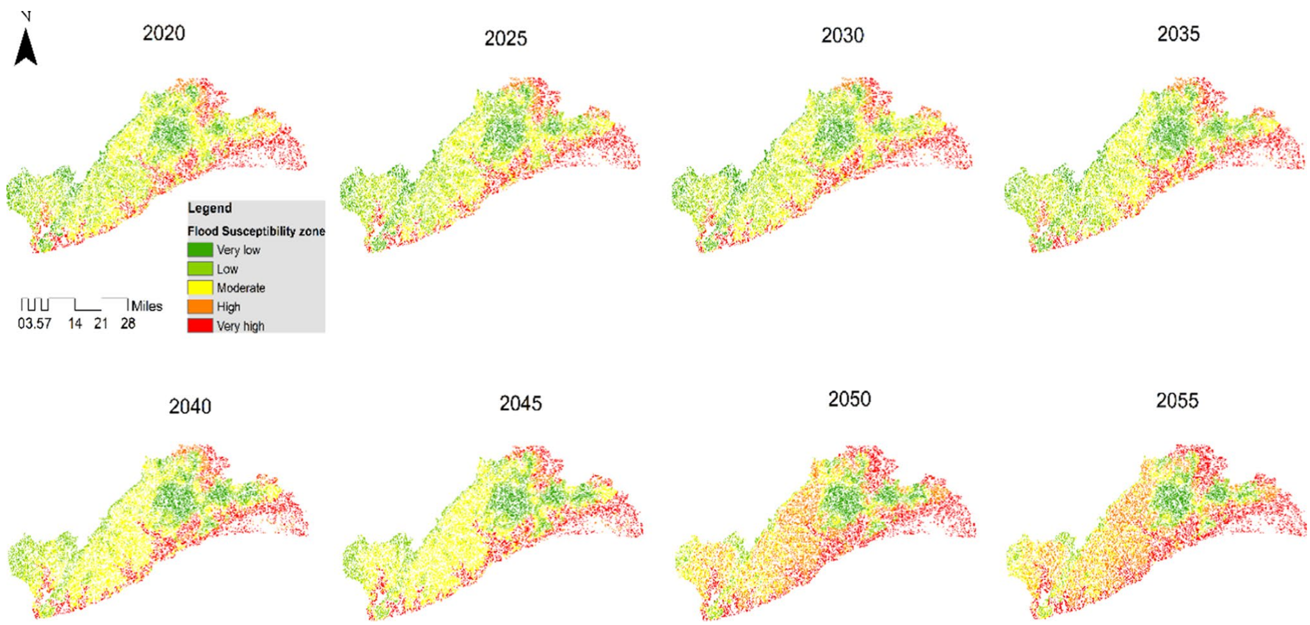


**Fig. 16** Spatio-temporal distribution of flood vulnerability zones under the SSP2 scenario

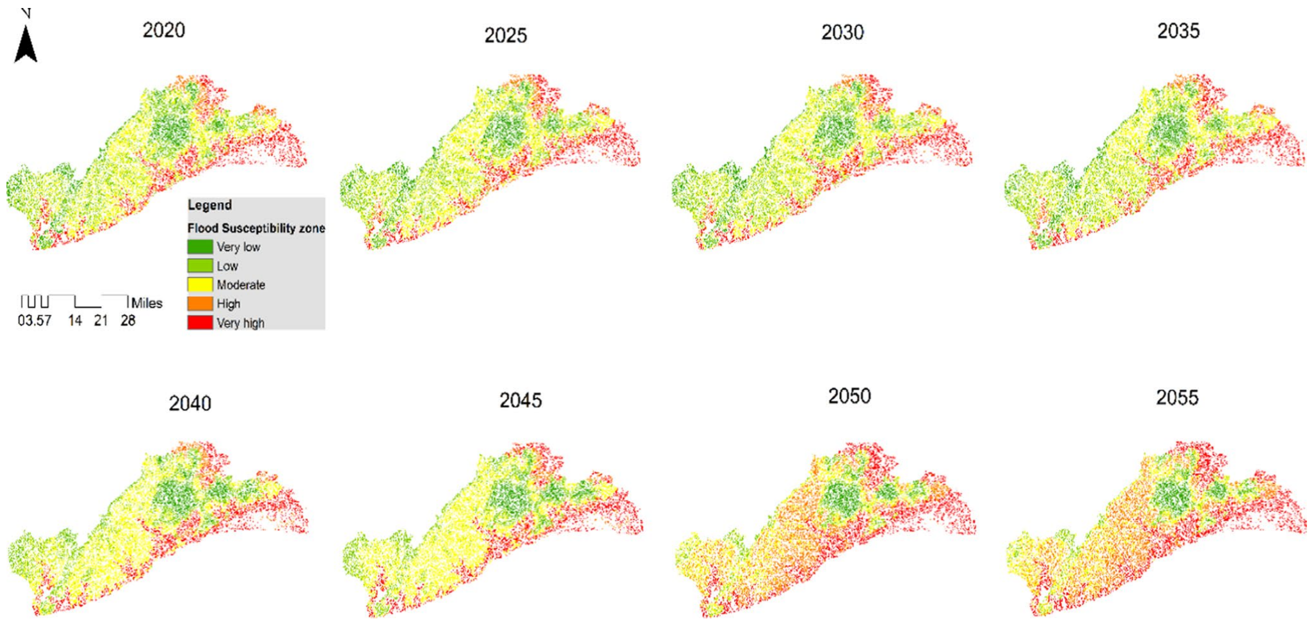


**Fig. 17** Spatio-temporal distribution of flood vulnerability zones under the SSP3 scenario

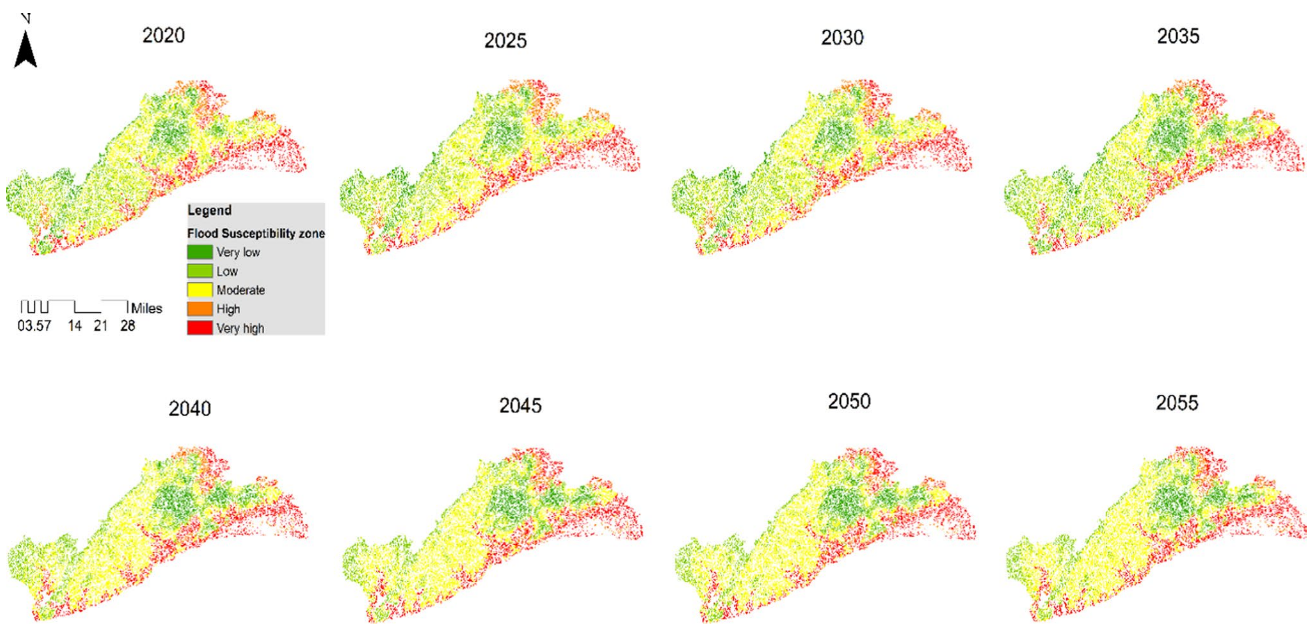


**Fig. 18** Spatio-temporal distribution of flood vulnerability zones under the SSP5 scenario

## Appendix 3: List of substations and their capacities

| Code | Bulk supply point name | Location | Capacity (MW) |
|---|---|---|---|
| A | Shiashi ECG Substation | Legon | 9.35 |
| B | ECG Sub Station—Exhibition | Dansoman Exhibition | 9.35 |
| C | ECG Substation | Teshie Nungua | 9.35 |
| D | ECG Korle-Bu | Korle Bu | 9.35 |
| E | ECG Substation Tema | Tema Steel Works | 9.35 |
| F | Enclave Power Company substation | Tema | 9.35 |
| G | Electricity Company of Ghana Substation | Ofankor | 9.35 |
| H | GRIDCO ACCRA-EAST SUBSTATION | Accra East | 28.05 |
| I | GRIDCO—ACHIMOTA SUBSTATION | Achimota | 28.05 |
| J | E.C.G. Primary Station [Tokose Station Z] | Weija | 9.35 |
| K | ECG Substation, Airport City Substation | Airport | 9.35 |
| L | Gbawe ECG substation | Mallam | 9.35 |
| M | ECG substation 'AH' (Ministries) | Ridge | 9.35 |
| N | ECG Transformer Substation | Adenta | 9.35 |
| O | Dawhenya ECG Sub-Station | Dawhenya | 9.35 |
| P | Siemens Power Plant | Tema | 9.35 |
| Q | ECG Power Sub Station | Awoshie | 9.35 |
| R | AFIENYA BSP | Afienya | 28.05 |
| S | ECG Power Station | Legon | 9.35 |
| T | Station AE | Kwabenya | 9.35 |
| U | Makola station G | Makola | 9.35 |
| V | Station Y Bastona | Spintex, Batsona | 9.35 |
| W | GrIdco accra central | adabraka | 28.05 |
| X | Graphic road | graphic road | 9.35 |
| Y | Avenor | avenor station | 9.35 |
| Z | ECG Station R | Ridge | 9.35 |
| AA | AJ | Tradefair Tseaddo | 9.35 |
| AB | Station X | Osu Kuku hill | 9.35 |
| AC | AU | Cantoments | 9.35 |
| AD | A-ECG substation | Odorkor | 9.35 |
| AE | Station L | Burma Camp | 9.35 |
| AF | ECG substation AS | Kanda substation | 9.35 |
| AG | Station K | Switchback, cantoments | 9.35 |
| AH | ECG station SW | Sowutuom | 9.35 |
| AI | Station AP | Polo grounds | 9.35 |
| AJ | Station F | Kokomlemle | 9.35 |
| AK | ECG substation AW | Awudome | 9.35 |
| AL | ECG substation S | Kwashieman | 9.35 |
| AM | ECG substation AL | Darkuman | 9.35 |
| AN | ECG substation A | Odorkor | 9.35 |
| AO | ECG substation AN | GIMPA | 9.35 |
| AP | Station Q | Tema—Meridian | 9.35 |
| AQ | Station A | TdC | 9.35 |
| AR | Station B | Comm 12 | 9.35 |
| AS | Station C | Comm 25 | 9.35 |

## References


1. Asumadu Sarkodie S, Owusu PA, Rufangura P. Impact analysis of flood in Accra, Ghana. Adv Appl Sci Res. 2015;6:53–78. https://doi.org/10.6084/M9.FIGSHARE.3381460.
2. Youssef B, et al. The contribution of the frequency ratio model and the prediction rate for the analysis of landslide risk in the Tizi N'tichka area on the national road (RN9) linking Marrakech and Ouarzazate. CATENA. 2023;232: 107464. https://doi.org/10.1016/j.catena.2023.107464.
3. Shafapour Tehrany M, Shabani F, Neamah Jebur M, Hong H, Chen W, Xie X. GIS-based spatial prediction of flood prone areas using standalone frequency ratio, logistic regression, weight of evidence and their ensemble techniques. Geomat Nat Hazards Risk. 2017;8(2):1538–61. https://doi.org/10.1080/19475705.2017.1362038.
4. Sarkar D, Mondal P. Flood vulnerability mapping using frequency ratio (FR) model: a case study on Kulik river basin, Indo-Bangladesh Barind region. Appl Water Sci. 2020;10(1):17. https://doi.org/10.1007/s13201-019-1102-x.
5. Billa L, Shattri M, Rodzi Mahmud A, Halim Ghazali A. Comprehensive planning and the role of SDSS in flood disaster management in Malaysia. Disaster Prev Manag Int J. 2006;15(2):233–40. https://doi.org/10.1108/09653560610659775.
6. Yu JJ, Qin XS, Larsen O. Joint Monte Carlo and possibilistic simulation for flood damage assessment. Stoch Environ Res Risk Assess. 2013;27(3):725–35. https://doi.org/10.1007/s00477-012-0635-4.
7. Messner F, Meyer V. Flood damage, vulnerability and risk perception—challenges for flood damage research. In: Flood risk management: hazards, vulnerability and mitigation measures. 2006. p. 149–167. Dordrecht: Springer Netherlands.
8. Rahmati O, Haghizadeh A, Pourghasemi HR, Noormohamadi F. Gully erosion susceptibility mapping: the role of GIS-based bivariate statistical models and their comparison. Nat Hazards. 2016;82(2):1231–58. https://doi.org/10.1007/s11069-016-2239-7.
9. Rahmati O, Pourghasemi HR, Zeinivand H. Flood susceptibility mapping using frequency ratio and weights-of-evidence models in the Golastan Province, Iran. Geocarto Int. 2016;31(1):42–70. https://doi.org/10.1080/10106049.2015.1041559.
10. Flash flood program. A compilation of 20 20–20 21 global flood events and international experience in flood management. 2022.
11. Few R. Flooding, vulnerability and coping strategies: local responses to a global threat. Prog Dev Stud. 2003;3(1):43–58. https://doi.org/10.1191/1464993403ps049ra.
12. Tschakert P, Sagoe R, Ofori-Darko G, Codjoe SN. Floods in the Sahel: an analysis of anomalies, memory, and anticipatory learning. Clim Change. 2010;103(3):471–502. https://doi.org/10.1007/s10584-009-9776-y.
13. Douglas I, Alam K, Maghenda M, Mcdonnell Y, Mclean L, Campbell J. Unjust waters: climate change, flooding and the urban poor in Africa. Environ Urban. 2008;20(1):187–205. https://doi.org/10.1177/0956247808089156.
14. BBC news. Million hit by floods in Africa. 2007. Accessed December 06, 2023. [Online]. Available: http://news.bbc.co.uk/2/hi/africa/6998651.stm#anchor
15. Amangabara GT, Obenade M. Flood vulnerability assessment of Niger Delta States relative to 2012 flood disaster in Nigeria. Am J Environ Prot. 2015;3(3):76–83.
16. Karley NK. Flooding and physical planning in urban areas in West Africa: situational analysis of Accra, Ghana. Theor Empir Res Urban Manag. 2009;4(4):25–41.
17. Twumasi YA, Asomani-Boateng R. Mapping seasonal hazards for flood management in Accra, Ghana using GIS. In: IEEE international geoscience and remote sensing symposium. 2002; Vol. 5, p. 2874–6. IEEE.
18. Rain D, Engstrom R, Ludlow C, Antos S. Accra Ghana: A city vulnerable to flooding and drought-induced migration. Case study prepared for cities and climate Change: Global Report on Human Settlements. 2011;2011:1–21.
19. Amoako C, Frimpong Boamah E. The three-dimensional causes of flooding in Accra, Ghana. Int J Urban Sustain Dev. 2015;7(1):109–29.
20. Perera ATD, Nik VM, Scartezzini J-L. Impacts of extreme climate conditions due to climate change on the energy system design and operation. Energy Proc. 2019;159:358–63. https://doi.org/10.1016/j.egypro.2019.01.002.
21. Entriken R, Lordan R. Impacts of extreme events on transmission and distribution systems. In:2012 IEEE Power and Energy Society General Meeting. 2012, p. 1–10. IEEE.
22. Xia J, Xu F, Huang G. Research on power grid resilience and power supply restoration during disasters—a review. Flood Impact Mitigation and Resilience Enhancement. 2020:8.
23. Wassmer J, Merz B, Marwan N. Resilience of emergency infrastructure networks after flooding events. In:EGU General Assembly Conference Abstracts. 2023. p. EGU-1383.
24. Kayaga SM, et al. Cities and extreme weather events: impacts of flooding and extreme heat on water and electricity services in Ghana. Environ Urban. 2021;33(1):131–50. https://doi.org/10.1177/0956247820952030.
25. Ali SA, Khatun R, Ahmad A, Ahmad SN. Application of GIS-based analytic hierarchy process and frequency ratio model to flood vulnerable mapping and risk area estimation at Sundarban region, India. Model Earth Syst Environ. 2019;5(3):1083–102. https://doi.org/10.1007/s40808-019-00593-z.
26. Khosravi K, Nohani E, Maroufinia E, Pourghasemi HR. A GIS-based flood susceptibility assessment and its mapping in Iran: a comparison between frequency ratio and weights-of-evidence bivariate statistical models with multi-criteria decision-making technique. Nat Hazards. 2016;83(2):947–87. https://doi.org/10.1007/s11069-016-2357-2.
27. Dewan AM, Islam MM, Kumamoto T, Nishigaki M. Evaluating flood hazard for land-use planning in greater Dhaka of Bangladesh using remote sensing and GIS techniques. Water Resour Manag. 2007;21(9):1601–12. https://doi.org/10.1007/s11269-006-9116-1.
28. Haq M, Akhtar M, Muhammad S, Paras S, Rahmatullah J. Techniques of Remote Sensing and GIS for flood monitoring and damage assessment: a case study of Sindh province, Pakistan. Egypt J Remote Sens Space Sci. 2012;15(2):135–41. https://doi.org/10.1016/j.ejrs.2012.07.002.
29. Lee MJ, Kang JE, Jeon S. Application of frequency ratio model and validation for predictive flooded area susceptibility mapping using GIS. In: 2012 IEEE international geoscience and remote sensing symposium. 2012. p. 895–8. IEEE.
30. Kwang C, Osei EM. Accra flood modelling through application of geographic information systems (gis). Remote Sensing Techniques and Analytical Hierarchy Process. J Remote Sensing & GIS. 2017;6(191):2.

31. Kumi-Boateng B, Peprah M, Larbi E. The integration of analytical hierarchy process (AHP), fuzzy analytical hierarchy process (FAHP), and Bayesian belief network (BBN) for flood prone areas identification—a case study of the Greater Accra Region, Ghana. J Geomat. 2020;14(2):100–22.
32. Yiran GAB, Kwang C, Blagogie L. Optimizing flood risk modelling with high-resolution remote sensing data and analytic hierarchy process. SN Soc Sci. 2024;4(6):111. https://doi.org/10.1007/s43545-024-00909-6.
33. Yilmaz OS. Flood hazard susceptibility areas mapping using Analytical Hierarchical Process (AHP), Frequency Ratio (FR) and AHP-FR ensemble based on Geographic Information Systems (GIS): a case study for Kastamonu, Türkiye. Acta Geophys. 2022;70(6):2747–69. https://doi.org/10.1007/s11600-022-00882-9.
34. Waseem M, Ahmad S, Ahmad I, Wahab H, Leta MK. Urban flood risk assessment using AHP and geospatial techniques in swat Pakistan. SN Appl Sci. 2023;5(8):215. https://doi.org/10.1007/s42452-023-05445-1.
35. Danso SY, Ma Y, Osman A, Addo IY. Integrating multi-criteria analysis and geospatial applications for mapping flood hazards in Sekondi-Takoradi Metropolis, Ghana. J Afr Earth Sci. 2024;209: 105102. https://doi.org/10.1016/j.jafrearsci.2023.105102.
36. Nkonu RS, Antwi M, Amo-Boateng M, Dekongmen BW. GIS-based multi-criteria analytical hierarchy process modelling for urban flood vulnerability analysis, Accra Metropolis. Nat Hazards. 2023;117(2):1541–68. https://doi.org/10.1007/s11069-023-05915-0.
37. Sezer EA, Pradhan B, Gokceoglu C. Manifestation of an adaptive neuro-fuzzy model on landslide susceptibility mapping: Klang valley, Malaysia. Expert Syst Appl. 2011;38(7):8208–19. https://doi.org/10.1016/j.eswa.2010.12.167.
38. Tiwari MK, Chatterjee C. Uncertainty assessment and ensemble flood forecasting using bootstrap based artificial neural networks (BANNs). J Hydrol. 2010;382(1):20–33. https://doi.org/10.1016/j.jhydrol.2009.12.013.
39. Chen Y-R, Yeh C-H, Yu B. Integrated application of the analytic hierarchy process and the geographic information system for flood risk assessment and flood plain management in Taiwan. Nat Hazards. 2011;59(3):1261–76. https://doi.org/10.1007/s11069-011-9831-7.
40. Samanta RK, Bhunia GS, Shit PK, Pourghasemi HR. Flood susceptibility mapping using geospatial frequency ratio technique: a case study of Subarnarekha River Basin, India. Model Earth Syst Environ. 2018;4(1):395–408. https://doi.org/10.1007/s40808-018-0427-z.
41. Pradhan B. Landslide susceptibility mapping of a catchment area using frequency ratio, fuzzy logic and multivariate logistic regression approaches. J Indian Soc Remote Sens. 2010;38:301–20.
42. Panchal S, Shrivastava AK. A comparative study of frequency ratio, Shannon's entropy and analytic hierarchy process (AHP) models for landslide susceptibility assessment. ISPRS Int J Geo-Inf. 2021;10(9):603. https://doi.org/10.3390/ijgi10090603.
43. Wang Q, Li W. A GIS-based comparative evaluation of analytical hierarchy process and frequency ratio models for landslide susceptibility mapping. Phys Geogr. 2017;38(4):318–37. https://doi.org/10.1080/02723646.2017.1294522.
44. Sharma S, Mahajan AK. A comparative assessment of information value, frequency ratio and analytical hierarchy process models for landslide susceptibility mapping of a Himalayan watershed, India. Bull Eng Geol Environ. 2019;78(4):2431–48. https://doi.org/10.1007/s10064-018-1259-9.
45. Dekongmen BW, et al. Flood vulnerability assessment in the Accra Metropolis, southeastern Ghana. Appl Water Sci. 2021;11(7):134. https://doi.org/10.1007/s13201-021-01463-9.
46. Nyarko BK. Flood risk zoning of Ghana: Accra experience. Part B, p. 12, 2002.
47. Adjei-Darko P. Remote sensing and geographic information systems for flood risk mapping and near real-time flooding extent assessment in the greater Accra metropolitan area. 2017.
48. Atakorah GB, Owusu AB, Adu-Boahen K. Geophysical assessment of flood vulnerability of Accra Metropolitan Area, Ghana. Environ Sustain Indic. 2023;19: 100286. https://doi.org/10.1016/j.indic.2023.100286.
49. Njomaba E, Ofori J, Aikins BE, Nyame DA. Flood risk mapping and its effects on livelihood in ghana using sentinel-1 data. a case study of accra. Int J Res Sci Innov. 2021;8(1).
50. GSS. Ghana 2021 Population and Housing Census General Report. 2021.
51. Siabi EK, et al. Assessment of Shared Socioeconomic Pathway (SSP) climate scenarios and its impacts on the Greater Accra region. Urban Clim. 2023;49: 101432. https://doi.org/10.1016/j.uclim.2023.101432.
52. Liu X, Li X, Liang X. A future land use simulation model by coupling human and natural effects. 2018.
53. Haklay M, Weber P. Openstreetmap: user-generated street maps. IEEE Pervasive Comput. 2008;7(4):12–8.
54. Choubin B, Moradi E, Golshan M, Adamowski J, Sajedi-Hosseini F, Mosavi A. An ensemble prediction of flood susceptibility using multivariate discriminant analysis, classification and regression trees, and support vector machines. Sci Total Environ. 2019;651:2087–96. https://doi.org/10.1016/j.scitotenv.2018.10.064.
55. Meraj G, Romshoo SA, Yousuf AR, Altaf S, Altaf F. Assessing the influence of watershed characteristics on the flood vulnerability of Jhelum basin in Kashmir Himalaya. Nat Hazards. 2015;77(1):153–75. https://doi.org/10.1007/s11069-015-1605-1.
56. Tehrany MS, Kumar L. The application of a Dempster–Shafer-based evidential belief function in flood susceptibility mapping and comparison with frequency ratio and logistic regression methods. Environ Earth Sci. 2018;77(13):490. https://doi.org/10.1007/s12665-018-7667-0.
57. Rahmati O, Pourghasemi HR. Identification of critical flood prone areas in data-scarce and ungauged regions: a comparison of three data mining models. Water Resour Manag. 2017;31(5):1473–87. https://doi.org/10.1007/s11269-017-1589-6.
58. Khosravi K, et al. A comparative assessment of flood susceptibility modeling using multi-criteria decision-making analysis and machine learning methods. J Hydrol. 2019;573:311–23. https://doi.org/10.1016/j.jhydrol.2019.03.073.
59. Haghizadeh A, Siahkamari S, Haghiabi AH, Rahmati O. Forecasting flood-prone areas using Shannon's entropy model. J Earth Syst Sci. 2017;126(3):39. https://doi.org/10.1007/s12040-017-0819-x.
60. Manandhar B. Flood plain analysis and risk assessment of Lothar Khola. Master of Science Thesis in Watershed Management. Tribhuvan University Institute of Forestry Pokhara, Nepal. 2010.
61. OCHA Situation Report on floods in Ghana No.1 | OCHA. Accessed: December 16, 2023. [Online]. Available: https://www.unocha.org/publications/report/ghana/ocha-situation-report-floods-ghana-no1
62. Jaafari A, Najafi A, Pourghasemi HR, Rezaeian J, Sattarian A. GIS-based frequency ratio and index of entropy models for landslide susceptibility assessment in the Caspian forest, northern Iran. Int J Environ Sci Technol. 2014;11(4):909–26. https://doi.org/10.1007/s13762-013-0464-0.

63. Regmi AD, et al. Application of frequency ratio, statistical index, and weights-of-evidence models and their comparison in landslide susceptibility mapping in Central Nepal Himalaya. Arab J Geosci. 2014;7(2):725–42. https://doi.org/10.1007/s12517-012-0807-z.
64. Lee S, Talib JA. Probabilistic landslide susceptibility and factor effect analysis. Environ Geol. 2005;47:982–90.
65. Sujatha ER, Rajamanickam V, Kumaravel P, Saranathan E. Landslide susceptibility analysis using probabilistic likelihood ratio model—a geospatial-based study. Arab J Geosci. 2013;6(2):429–40. https://doi.org/10.1007/s12517-011-0356-x.
66. Akgun A, Dag S, Bulut F. Landslide susceptibility mapping for a landslide-prone area (Findikli, NE of Turkey) by likelihood-frequency ratio and weighted linear combination models. Environ Geol. 2008;54(6):1127–43. https://doi.org/10.1007/s00254-007-0882-8.
67. Mondal S, Maiti R. Integrating the Analytical Hierarchy Process (AHP) and the frequency ratio (FR) model in landslide susceptibility mapping of Shiv-khola watershed, Darjeeling Himalaya. Int J Disaster Risk Sci. 2013;4(4):200–12. https://doi.org/10.1007/s13753-013-0021-y.
68. Fan J, Upadhye S, Worster A. Understanding receiver operating characteristic (ROC) curves. Can J Emerg Med. 2006;8(1):19–20.
69. Climate Guide. Accra climate: weather by month, temperature, rain—Climates to Travel. Accessed: Oct. 21, 2023. [Online]. Available: https://www.climatestotravel.com/climate/ghana/accra
70. Ansah SO, et al. Meteorological analysis of floods in Ghana. Adv Meteorol. 2020;2020: e4230627. https://doi.org/10.1155/2020/4230627.
71. USGS. Precipitation and the Water Cycle | U.S. Geological Survey. Accessed: October 21, 2023. [Online]. Available: https://www.usgs.gov/special-topics/water-science-school/science/precipitation-and-water-cycle
72. Samir K, Wolfgang L. The human core of the shared socioeconomic pathways: population scenarios by age, sex and level of education for all countries to 2100. Glob Environ Change. 2017;42:181–92. https://doi.org/10.1016/j.gloenvcha.2014.06.004.
73. Asumadu-Sarkodie S. Situational analysis of flood and drought in Rwanda. Int J Sci Eng Res. 2015;6(8):960–70. https://doi.org/10.14299/ijser.2015.08.013.
74. Bach B, Cotter C, Lepine M, Regan S. Storm surge & critical infrastructure on Nantucket. 2015.
75. Boggess JM, Becker GW, Mitchell MK. Storm & flood hardening of electrical substations. In: 2014 IEEE PES t&d conference and exposition. 2014. p. 1–5. IEEE.
76. Saadeghvaziri MA, Feizi B, Kempner Jr L, Alston D. On seismic response of substation equipment and application of base isolation to transformers. IEEE Trans Power Deliv. 2009;25(1):177–86.
77. Kim GH, Lee JY, Bae SM. The development of a flood protection system for pad transformers using pneumatic pressure in areas prone to floods. 조명· 전기설비학회논문지. 2010;24(3):27–32.
78. Betancourt-Ramirez E, Ndiaye I, Castellanos-Gonzalez J. Grid-ready flexible transformers for resilient transmission networks. In: 2022 7th international advanced research workshop on transformers (ARWtr) 2022. p. 103–8. IEEE.
79. Panteli M, Trakas DN, Mancarella P, Hatziargyriou ND. Power systems resilience assessment: hardening and smart operational enhancement strategies. Proc IEEE. 2017;105(7):1202–13. https://doi.org/10.1109/JPROC.2017.2691357.